4-2005

Copper Exchange Studies between the First and Fourth N-Terminal Metal-Binding Domains of Wilson Disease ATPase

Jennifer Bunce

COPPER EXCHANGE STUDIES BETWEEN THE FIRST AND FOURTH N-TERMINAL METAL-BINDING DOMAINS OF WILSON DISEASE ATPASE

by

Jennifer Bunce

A Thesis
Submitted to the
Faculty of The Graduate College
in partial fulfillment of the
requirements for the
Degree of Master of Science
Department of Chemistry

Western Michigan University
Kalamazoo, Michigan
April 2005

ACKNOWLEDGMENTS

I would like to express my gratitude to Dr. David Huffman for providing me with this research opportunity and supplying insightful advice concerning this project. I would also like to thank Dr. Jonathan Gitlin of University of Washington University at St. Louis for donating the plasmid containing the full-length ATP7B gene, Dr. Todd Barkman's lab group for generously sequencing all potential plasmid constructs, and Saman Shafaie of Northwestern University for his ICP-MS expertise. Lastly, I would like to thank the Chemistry Department of Western Michigan University for this learning experience.

Jennifer Bunce

COPPER EXCHANGE STUDIES BETWEEN THE FIRST AND FOURTH N-TERMINAL METAL-BINDING DOMAINS OF WILSON DISEASE ATPASE

Jennifer Bunce, M.S.

Western Michigan University, 2005

The human copper-transporting ATPase Wilson's disease protein was one of the first proteins shown to be actively involved in cellular copper homeostasis. The protein includes six N-terminal metal binding domains. The individual capabilities of the domains to bind and transfer copper are not yet fully understood. Each metal-binding domain is about 72 amino acid residues long and contains the conserved binding motif GMTCXXC, of which the cysteines are involved in the copper coordination. Studies have shown that the protein binds six copper atoms suggesting the potential involvement of each metal-binding domain. Separate functional roles for the latter domains have been proposed implicating a possible interaction between the domains.

Here the first and fourth domains have been isolated and characterized by several chemical means including high resolution gel filtration, MALDI mass spectroscopy, and isoelectric focusing. Each domain demonstrated copper binding capabilities. Copper exchange activity has demonstrated between the two individual metal-binding domains *in vitro* using varying molar ratios between donor and acceptor. The exchange event was determined to be reversible and equilibrium was quickly achieved in less than 5 minutes. The $K_{exchange}$ constant is estimated at 0.69 for the reaction.

TABLE OF CONTENTS

Table of Contents—continued

Table of Contents—continued

LIST OF TABLES

LIST OF FIGURES

CHAPTER I

INTRODUCTION

Copper Homeostasis

Copper is an essential trace metal required by both prokaryotes and eukaryotes (Linder, 1991). Many metalloenzymes require copper as a catalytic cofactor in various redox reactions. Some of these enzymes and their associated biological functions include cytochrome c oxidase for oxidative metabolism, dopamine monooxygenase for neurotransmitter synthesis, superoxide dismutase for free radical detoxification, ceruloplasmin for iron uptake, and lysl oxidase for maturation of connective tissue (Danks, 1995). While the nutrient requirement of copper is essential, excess copper is toxic (Vulpe, 1995). As a transition metal, copper is able to participate in reactions which generate reactive oxidative species (ROS). ROS cause oxidative damage to biological molecules such as proteins, lipids, and nucleic acids. Consequently, intracellular copper concentrations must be stringently regulated to ensure bioavailability to essential enzymes while preventing accumulation to toxic levels.

Recent studies, employing yeast as a eukaryotic model system, suggested the intracellular free copper concentration to be less than one atom per cell necessitating a copper carrier for transport to target proteins (Rae, 1999). The lack of "free" copper ion quantities is due to an overcapacity to chelate copper within the cell. For this reason, there are several copper receptors which function to facilitate the transport of copper to selective proteins. These copper receptors are part of a class of proteins called metallochaperones (Pufahl, 1997). Several metallochaperones have

evolved to form specific pathways for the proper trafficking of copper within cells (O'Halloran, 2000). Metallochaperones function to bind and protect metals from intracellular chelation and non-specific binding during their conveyance and ensuing transfer to specific partner proteins. In addition to copper chaperones, copper-transporting P-type ATPases play an important role in copper trafficking. P-Type ATPases are membrane-bound heavy metal transporters responsible for the active transport of cations across cell membranes. ATPases hydrolyze ATP to drive the metal transport process resulting in either metal uptake or efflux. Studies have shown that these copper trafficking proteins, both metallochaperones and P-type ATPases, are highly conserved across species and homologs have been identified in bacteria, yeast, plants, and mammals (Arnesano, 2001b; Rosenzweig, 2001; Solioz, 1994).

Overview of Copper Metabolism

Presented is an outline of a proposed model for copper metabolism at the cellular level as illustrated in Figure 1 (review Peña, 1999; review Camakaris, 1999). Estimates of human daily dietary intake of copper range from 0.6 to 1.6 mg per day (Linder, 1996). Predominantly this copper is absorbed from the cells lining the stomach and the small intestine. Copper must first be reduced from the assumed Cu(II) oxidation state to Cu (I) before entering the cell and this event is thought to take place either prior to or during uptake by a hypothetical reductase. Uptake of copper into cells occurs via a high affinity permease, hCtr1 (Puig, 2002; Lee, 2002). In the cytoplasm, copper is bound by copper chaperones which shuttle the metal to specific target proteins. Important cuproproteins are located within multiple endoplasmic reticulum, and secretory vesicles. Several distinct pathways of copper trafficking have been established (review O'Halloran, 2000). Examples of this

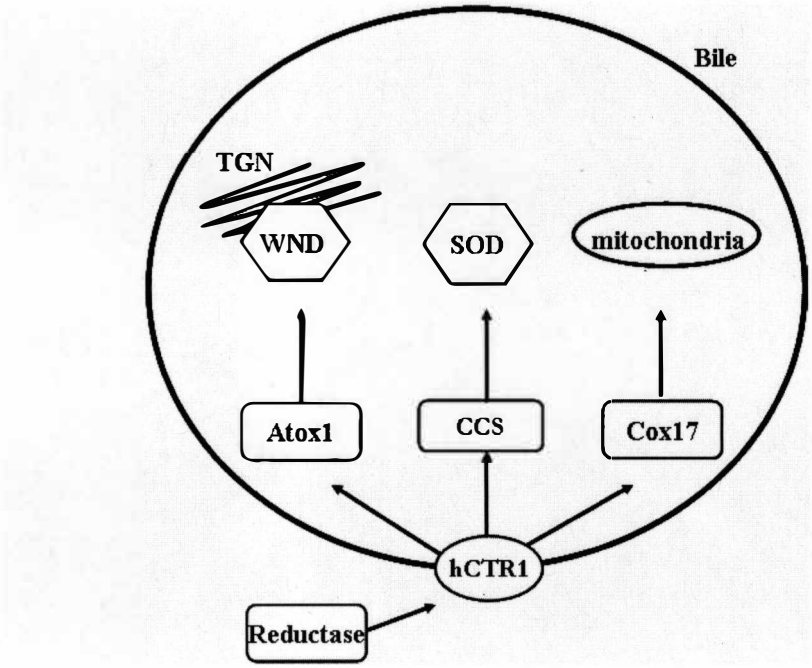

Figure 1. Model of Cellular Copper Metabolism

specific copper distribution by metallochaperones include (a) hCOX17 shuttling of copper to the mitochondria (Amaravadi, 1997), essential for incorporation of copper into the enzyme cytochrome c oxidase, (b) Ccs1 copper delivery to SOD1 (Culotta, 1997), a Cu/Zn superoxide dismutase, and (c) Atox1 transporting copper to the secretory pathway (Klomp, 1997) via interaction with the copper-transporting ATPases Wilson disease protein (WDP) or Menkes disease protein (MNK).

Human Genetic Defects in Copper Transport

The discovery of the genes responsible for the two genetic disorders associated with defects in copper metabolism, Menkes (Vulpe, 1993) and Wilson's (Bull, 1993) diseases has generated renewed interest in the molecular mechanisms of copper transport.

Menkes Disease

Menkes disease is an X-linked recessive disorder characterized by severe copper deficiency due to reduction of dietary copper absorption (Menkes, 1962). Patients with Menkes disease exhibit neurodegeneration, developmental complications, connective tissue abnormalities, and usually do not survive past early childhood (Menkes, 1962). These symptoms are a result of the lack of copper incorporation into several developmentally important cuproproteins (Danks, 1972).

The disease arises from mutations in the gene encoding for the P-type ATPase, named ATP7A. ATP7A has been genetically mapped to the q13 region of the X-chromosome and encodes a protein consisting of 1500 amino acid residues (Vulpe, 1993). Menkes disease protein (MNK) transports copper into the secretory pathway of the gastrointestinal tract, placenta, and blood-brain barrier (review Danks, 1995). MNK is also responsible for exporting copper from other tissues notably, the intestinal mucosa (review Danks, 1995). MNK is highly expressed in most tissues with the exception of the liver (Vulpe, 1993; Paynter, 1994). Accordingly, mutations of the MNK gene result in copper accumulation in those tissues where ATP7A is highly expressed specifically the kidney, duodenum, and placenta, while a severe copper deficiency develops in most other tissues.

Wilson's Disease

Wilson's disease is an autosomal recessive disorder of copper homeostasis distinguished by increased copper accumulation in the liver, kidneys, and brain (Wilson, 1912). Patients exhibit symptoms of liver cirrhosis, renal dysfunction, and neuronal degeneration (Brewer, 1992). Many patients are diagnosed by the characteristic Kayser-Fleischer rings visible on the cornea (Kayser, 1902; Fleischer,

1903). At the cellular level the disease is characterized by a failure of hepatocytes to incorporate copper into the ceruloplasmin (Scheinberg, 1952) and a marked decrease of copper excretion in the bile (Suzuki, 1994; Terada, 1999).

Wilson's disease is caused by mutations in the gene encoding for the P-type ATPase ATP7B, a gene highly homologous to ATP7A in structure and function (Bull, 1993). ATP7B is located on chromosome 13 at q14.3 and comprises 80 kb of genomic DNA and 21 exons. The P-type ATPase protein produced is 1411 amino acid residues long (Yamaguchi, 1993).

Wilson disease protein (WDP) is expressed primarily in the liver, secondarily in the kidneys, and to a lesser degree in the brain, heart, and lungs (Bull, 1993). Most dietary copper is deposited in the liver where the production of bile occurs; bile is a primary excretion pathway for copper (Linder, 1991). WDP is located within the trans-Golgi network and is essential for incorporating copper into ceruloplasmin (Terada, 1998), a multicopper oxidase with ferroxidase activity that is the most abundant copper-binding protein in the blood plasma.

MNK and WDP Roles in Copper Transport

Although MNK shares a high homology level to WDP both in manners of structure and function, the two proteins are expressed in different tissues and thus serve different physiological roles. The means by which these two P-type ATPases contribute to copper homeostasis are not yet fully understood. Many recent studies have been published in an effort to elucidate the molecular mechanism for each protein. Several areas of interest exist concerning MNK and WDP. Among the most extensively examined topics are the protein structure, metal specificity, cellular localization, interaction with metallochaperone Atox1, distinguishing the roles of

different domains within the proteins, and regulation of protein catalytic activity by copper, external factors or self-regulation.

Conserved Domains in Copper-Transporting ATPases

The mechanisms of copper-transport for P-type ATPases are thought to be evolutionarily retained. An example of this mechanistic preservation is illustrated by complementation studies of MNK and WDP and their yeast homologue, Ccc2. Ccc2 provides copper to the Fet3p multicopper oxidase, a homologue of human ceruloplasmin (Yuan, 1995). MNK and WDP were each able to restore copper incorporation into Fet3p when expressed in a Ccc2 deficient yeast strain (Payne, 1998; Iida, 1998).

Significant structural motifs are conserved in all heavy-metal-transporting P-type ATPases with additional discerning traits for those ATPases specific for copper-transport (Bull, 1994; Lutsenko, 1995; Lieberman, 2004) an illustration of these conserved motifs is provided in Figure 2. Among these common features are the eight transmembrane domains, of which the sixth segment contains the highly conserved intramembrane sequence CPC. The conserved cysteines of the CPC motif are thought to serve as the metal-binding site during copper transport across the membrane. Specific to the copper-transporting ATPases but not all heavy-metal-transporting ATPases is the conserved sequence of YN located in the seventh transmembrane domain. P-type ATPases transporting other heavy metals such as zinc and cadmium lack this YN motif (Lutsenko, 2002). Recently this motif was determined to effect the copper coordination of the Cu-transporting P-type ATPase CopA using mutational analysis (Mandal, 2004).

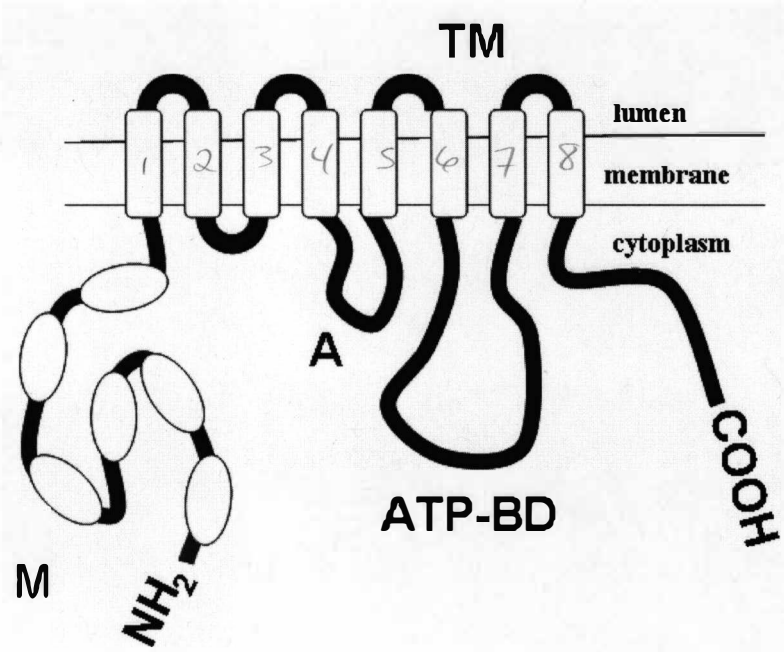

Figure 2. Generalized Structure of a Copper-transporting P-type ATPase

Copper-transporting ATPases are comprised of four major conserved domains: eight transmembrane segments (TM), an ATP-binding domain (ATP-BD), an actuator domain (A), and the one-six metal-binding N-terminus domains (M).

The remaining conserved domains of copper-transporting ATPases are found within the cytosolic loops of the membrane-bound protein. An ATP-binding site is situated in the loop between the sixth and seventh transmembrane domains Tsivkovskii, 2001). The ATP-binding site can be divided into two parts, a phosphorylation site, and a nucleotide binding site. The phosphorylation site is comprised of the invariant sequence DKTG, where the aspartic acid is phosphorylated during ATP hydrolysis. The nucleotide-binding site, containing conserved sequence SEHPL, is believed to bind adenine from ATP. Situated in the cytosolic loop between the fourth and fifth transmembrane domains lies the actuator

domain, sequence motif TGE. The actuator domain name alludes to its role of interacting with the ATP-binding site, a requisite for conformational changes to occur which are necessary for catalytic transport activity of the protein (Toyoshima, 2000). Intriguingly the most variability within the conserved domains of the copper-transporting ATPases is found in the N-terminal metal binding domains (MBDs). Although all copper-transporting ATPases have at least one metal-binding domain, they may contain as many as six MBDs. These MBDs each are approximately 70 amino acid residues in length, and possess the highly conserved metal-binding sequence GMTCXXC. A sequence alignment of the six MBDs of WDP is shown in Figure 3 with the conserved metal-binding region boxed. The conserved cysteines each contribute a metal binding ligand to complex copper. While the structures for most copper-transporting ATPases are as yet undetermined, recent NMR solution structures for select individual MBDs are available. Structures recently solved include those for MNK MBD2, apo and Cu (I)-bound forms (Banci, 2004), MNK MBD4, apo and Ag (I)-bound forms (Gitschier, 1998), and the first MBD of the yeast homolog Ccc2, apo and Cu (I)-bound forms (Banci, 2001). Homology models predict that N-MBDs share a conserved "ferrodoxin-like" βαββαβ fold (Arnesano, 2002). This fold motif is also predicted for copper chaperones containing the GMTCXXC binding site, since a high level of homology exists between these metallochaperones and the N-MBDs (Huffman, 2001). The solved structures for the human copper chaperone, Atox1 (Wernimont, 2000), for MNK and WDP and its yeast homolog, Atx1 (Arnesano, 2001a), also exhibit the βαββαβ fold. Figure 4 shows the copper bound MBD2 of MNK in comparison with the copper bound metallochaperone Atox1.

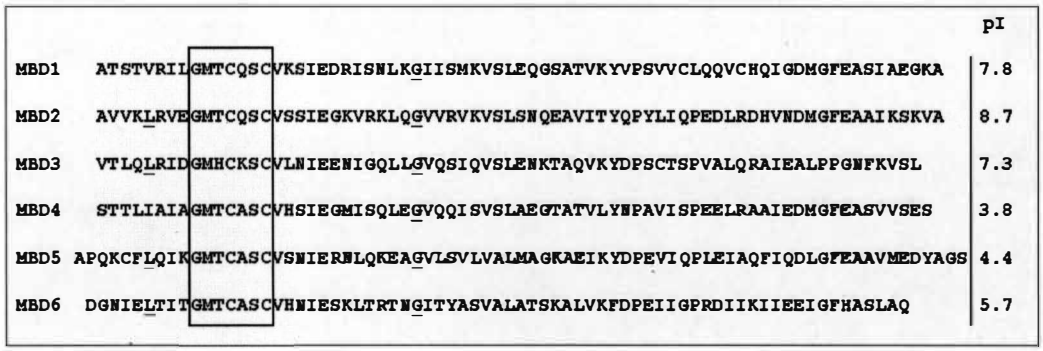

Figure 3. Sequence Alignment of the MBDs of WDP

Amino acid sequences of the six N-terminal MBDs of WDP as aligned by conserved metal binding motif identified above in the boxed region (Genbank protein sequence accession # P35670 [gi|1703455]. Three missence mutations located within the MBDs are known which cause Wilson disease to occur. These three mutations include (G85V) within MBD1, (L492S) within MBD5, and (G591D) within MBD6. The conserved glycine and leucine residues involved are underlined above. The predicted isoelectric points of the MBDs are provided (Huffman, 2001).

Prokaryotic and yeast homologues often have only one or two N-MBDs, whereas both MNK and WDP each have six. The increased number of MBDs found in higher species compared to prokaryotes and lower eukaryotes suggest that some of the MBDs of higher species may serve alternate functions other than transport activity. The MBDs of MNK and WDP might be differentiated in their functions, possibly serving to regulate the protein's activity rather than participating in transport activity or both.

Regulation of MNK and WDP Activity

Several regulatory factors, including copper itself, have been shown to be associated with the metabolic activities of MNK and WDP affecting such properties as copper binding, transport, and intracellular protein trafficking. Studies employing immunohistochemical techniques revealed that both MNK and WDP are localized to

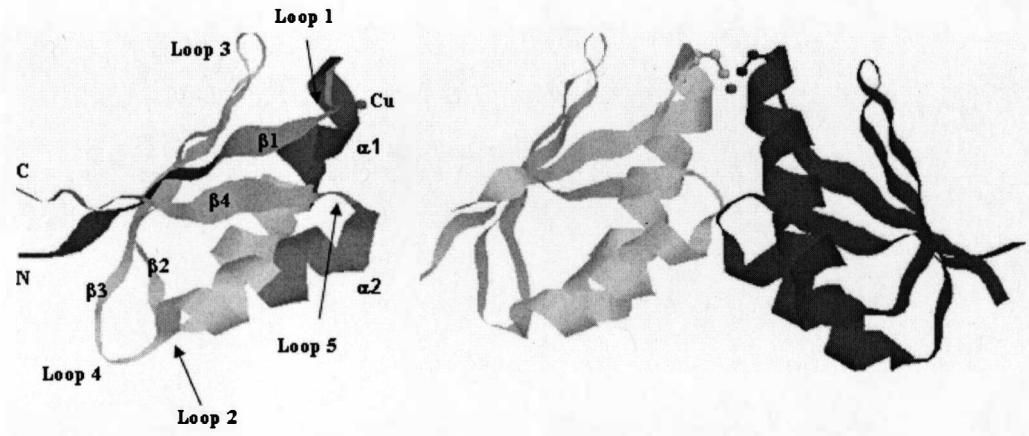

Figure 4. Conserved βαββαβ Fold Motif Observed in MNK MBDs and Metallochaperone Atox1

The NMR solution structure of Cu-MBD2 of MNK is shown above on the left (PDB entry: 1SQU) and the determined crystal structure of the copper bound homodimer of Atox1 (PDB entry: 1FEE) is shown above on the right. Both proteins have been shown to bind copper in a monomeric bicoordinate manner with two cysteine residues (Banci, 2004; Anastassopoulou, 2004). The two metal coordinating cysteine residues are located within loop 1 and the N-terminal end of the first alpha helix for each protein. Atox1 has also been shown to bind copper in a 3- or 4-coordinate manner as a homodimer (Wernimont, 2000). The conserved " ferrodoxin-like" βαββαβ fold motif is also predicted for the MBDs of WDP. Figure 4 was prepared using RASMOL.

the trans-Golgi network (TGN) under conditions of basal copper concentrations (Suzuki, 1999). These same studies also showed a reversible copper-induced trafficking event of both proteins from the TGN to cytoplasmic vesicles (Yamaguchi, 1996). In WDP, trafficking was also accompanied by an increase in copper excretion to the bile (Hung, 1997).

During the catalytic cycle of P-type ATPases an acyl-phosphorylated intermediate is produced prior to cation transport. In MNK and WDP this catalytic phosphorylation event is related to protein trafficking, given that it is also a copper dependent event (Petris, 2002; Vanderwerf, 2001).

The human copper chaperone Atox1 directly interacts with MNK and WDP for delivery of cytoplasmic copper to the secretory pathway (Larin, 1999; Hamza, 1999). Furthermore, apo Atox1 has been shown to be capable of removing copper from WDP (Walker, 2002). This signifies that both copper-bound and apo forms of Atox1 may participate in the regulation of WDP activity. Recently it has also been suggested that Atox1 influences the threshold at which copper-dependent events of MNK take place(Walker, 2002). Atox1-deficient cells exhibited diminished copper-dependent trafficking of MNK in comparison to wild type cells (Hamza, 2003). MNK copper-induced trafficking was restored upon overexpression of Atox1 or copper level elevation.

However the most extensively studied area, concerning the regulation of MNK and WDP activities, may be discerning the role of the N-MBDs. Many different functions have been associated with the N-MBDs of MNK and WDP. Several studies have shown that mutations of the N-MBDs of MNK and WDP hinder their ability to transport copper and rescue the function of copper incorporation into the yeast ceruloplasmin homologue, Fet3, within Ccc2 deficient yeast (Payne, 1998; Forbes, 1999). These studies illustrate the importance of the N-MBDs of MNK and WDP for copper translocation.

Moreover, Atox1 reversibly transfers copper specifically to the N-MBDs of MNK and WDP, revealing that the N-MBDs are essential for interaction with the copper chaperone as well as copper transport activity (Larin, 1999; Walker, 2002).

There is evidence that the copper-mediated trafficking of MNK is associated with its N-MBDs. Mutations of the N-MBDs of MNK result in inhibition of intracellular trafficking suggesting the MBDs may initiate this event through the effects of copper-binding (Strausak, 1999). The N-MBDs of WDP were determined to be responsible for the cooperative effect of copper on catalytic phosphorylation activity (Huster, 2003). While many aspects of how the N-MBDs of MNK and WDP affect copper transport, catalytic phosphorylation activity, copper chaperone interactions, and intracellular trafficking of the proteins, several issues remain unclear, especially the specific functions of the six N-MBDs.

Role of the N-terminal Metal-binding Domains

The precise functions of the six N-MBDs of WDP and MNK are still poorly understood. In many recent studies the six metal binding sites of MNK and WDP were found to be functionally non-equivalent within each protein. What's more, variations in function between the N-MBDs of MNK and WDP highlight that findings for one protein may not be applicable to the other.

Copper Translocation

An example of the functional differences between the individual MBDs of MNK and those of WDP can be found in their copper transport properties. Yeast complementation assays have demonstrated that the sixth MBD of WDP alone is sufficient for loading copper into Fet3, the yeast homologue of ceruloplasmin (Iida, 1998). A separate study found that the positioning of the sixth MBD as the most C-terminal domain could not account for the discrepancy between domains (Forbes, 1999). When the second and third MBDs were mutated in a manner such that their

position relative to the first transmembrane segment was equivalent to that of the MBD6 in the wild type, the mutants were still unable to restore copper transport. This suggests distinct functions for the individual domains of WDP and that the last two or three most C-terminal domains may be playing a more crucial role in copper transport.

In contrast to WDP, yeast complementation assays of MNK suggest the third MBD may play a critical role in copper transport (Payne, 1998). Successive mutations, beginning with the first MBD, resulted in a sudden termination of copper transport after the third mutation. However discrepancies have been reported as to whether the N-MBDs of MNK are even essential for copper translocation. Mutational studies in mammalian cells involving replacement of the metal coordinating cysteine residues with serine residues show that copper transport into the secretory pathway is reduced but still detectable even in the presence of mutated non-functional N-MBDs (Voskoboinik, 1999).

Copper-mediated Protein Trafficking

Both MBDs five and six were each found to be capable of singly redistributing WDP in the presence of elevated copper (Cater, 2004). The same study also reported that the first three MBDs of WDP could not functionally replace MBD5 and MBD6 for copper-induced intracellular protein trafficking. Mutational studies of the N-MBDs of MNK also report that only the fifth and sixth MBDs are necessary for copper-induced translocation from the TGN to the cytoplasmic vesicles (Strausak, 1999). These studies imply a conserved mechanism may exist between MNK and WDP regarding copper-mediated intracellular trafficking mechanisms.

Catalytic Phosphorylation Activity

Phosphorylation of P-type ATPases is contingent on copper binding to the CPC intramembrane site. Mutations of the N-MBDs of WDP suggest that the fifth and sixth MBDs play a pivotal role in regulating the protein's phosphorylation activity by affecting the affinity of the CPC intramembrane site for copper (Huster, 2003). The same studies also noted an increase in the copper dependence for the phosphorylation of the protein when the first four MBDs were mutated. The author suggests these first four MBDs may affect availability of copper to the catalytically important fifth and sixth domains thereby determining the regulating of the protein turnover. In support of this theory of conformationally mediated interaction, circular dichroism (CD) spectroscopy data shows that WDP undergoes metal-specific conformational changes with addition of increasing of amounts of copper (DiDonato, 2000). Another study using the N-terminal model of the rat equivalent of WDP, showed similar metal-induced secondary and tertiary structural changes (Tsay, 2004).

Atox1 Interaction

Yeast two-hybrid analysis of MNK and WDP interaction with the copper chaperone Atox1 show variances between the six N-MBDs of each protein (Larin, 1999; Strausak, 2003). For WDP the fifth and sixth MBDs failed to interact with Atox1 while the first four domains were each capable of independent interaction (Larin, 1999). More recently, a similar study was conducted examining the interaction of the individual N-MBDs of MNK with Atox1 (Strausak, 2003) comparing results obtained from yeast two-hybrid assays to results of surface plasmon resonance (SPR). It is noteworthy to point out that the yeast two-hybrid

assay results were similar to those of WDP, with the fifth and sixth MBDs of MNK failing to show interaction with Atox1 while SPR revealed a copper-dependent interaction of the chaperone with all six MBDs. A third study using yeast two-hybrid analysis to examine the interactions between the chaperone Atox1 and the individual MBDs of WDP detected copper-dependent interactions between the chaperone with MBD1, MBD2, and MBD4 with the largest relative strength of the MBD-chaperone interaction occurring with MBD4 (van Dongen, 2004). Further examination of the interactions between Atox1 and the individual MBDs of MNK or WDP is still needed to fully discern the interactions between MNK or WDP and Atox1. For each yeast two-hybrid analysis study the MBDs examined were cloned in a unique manner to differentiate the separate MBDs and determine their interactions. These methods include (a) mutationally altering the copper coordinating cysteine residues to serine (Strausak, 2003), (b) using deletion constructs (Larin, 1999), and (c) individual cloning of the MBDs (van Dongen, 2004).

Recent research has also examined whether Atox1 delivers copper to a preferential MBD of WDP. The transfer of a single copper from the chaperone to the N-MBD was performed followed by fluorescent labeling with the cysteine-directed probe 7-diethylamino-3-(4′-malemeimdylphenyl)-4-methylcoumarin (CPM). Next the labeled protein was subjected to proteolysis of the N-MBDs and subsequent amino acid sequencing of the digested fragments (Walker, 2004). Based upon previous work exhibiting the ability of copper-bound MBDs to selectively protect their own cysteine residues against labeling by CPM (Lutsenko, 1997), the authors suggest that MBD2 of WDP preferentially receives copper from Atox1 (Walker, 2004). However since the changes in fluorescent intensities are only offered in a

qualitative manner and are not actually quantified, the data presented is insufficient to determine whether MBD2 alone is shielded from CPM labeling.

Further investigations (Walker, 2004) did not display a selective shielding of the MBDs from CPM labeling when free copper was added to the N-MBDs indicating the Atox1 may be preferentially delivering copper to specific MBDs within WDP. Surface labeling experiments yielded similar results with no preferential copper-binding detected. For determination of whether MBD2 is essential for the delivery of copper to WDP, site-directed mutagenesis of MBD2's cysteine residues to alanine was performed and catalytic phosphorylation activity was monitored upon addition of either copper or Cu-Atox1. Free copper was able to reactivate catalytic phosphorylation in both the wild type and the mutant. When copper was delivered via Atox1, reactivation of catalytic phosphorylation activity was markedly lower in the mutant compared to the wild type. The author suggests MBD2 is important to the copper delivery event from the copper chaperone Atox1 to WDP (Walker, 2004). Mutational analysis of the other five MBDs of WDP was not performed therefore their importance regarding copper delivery remains unknown.

Additionally Walker et al. suggests that the copper bound to MBD2 does not transfer to the other MBDs and thus MBD2 is not acting as the metal loading entry point for the protein (Walker, 2004). When Cu-MBD2 was exposed to increasing quantities of the copper-chelator bicinchoninic acid (BCA) of up to 45-fold molar excess only 10% of copper was removed whereas similar studies conducted with Cu-Atox1 show a complete loss of copper to BCA. As opposed to a metal loading entry point role, Walker et al. suggest that copper binding to MBD2 may cause a conformational shift of WDP subsequently allowing the other MBDs to interact with Atox1. These conclusions are founded in the observation that different sized

fragments of WDP were generated by trypsin proteolysis after the transfer of a single copper to the protein therefore copper must cause a conformational change exposing new sites for trypsin digestion.

Copper Coordination and Exchange

Metal Ion Specificity

Although a high level of sequence similarity exists among P_1-type ATPases, a subclass of P-type ATPases transporting heavy metals, numerous studies have shown these proteins are very selective for the metal ions transported. ZntA is a P_1-type ATPase specific for Pb(II), Zn(II), Cd(II), and Hg(II) containing one GXXCXXC sequence whereas WDP is specific for Cu(I) and possibly Ag(I) and contains six repeats of the GXXCXXC motif (Hou, 2001). Previously, the issue of whether the N-terminal metal binding region of ZntA was essential for metal ion discrimination in the protein was examined using a truncated mutant lacking the amino terminal domain (Mitra, 2001). The ZntA mutant was still able to confer metal ion specificity without the presence of the metal binding domain from which the authors concluded that the transmembrane segments of the protein were primarily responsible for metal ion recognition.

Additional experiments were conducted using chimeric proteins of ZntA in which either its N-MBD was replaced with the whole N-terminal domain of WDP, or only MBD6 of WDP (Hou, 2001). The chimeras of ZntA were each able to confer resistance to lead, zinc, and cadmium salts but not copper salts. Both chimeras also displayed ATPase activity in the presence of lead, zinc, cadmium, and mercury, all of which are ZntA substrates, but none such activity was detected for copper or silver, the metal substrates of WDP.

While the truncated mutants and chimeras of ZntA both retained metal ion specificity, a reduction in ATPase activity compared to wild type ZntA was observed for each case (Hou, 2001). These results suggest that replacing the N-terminal domain of ZntA may not alter the protein's metal specificity determined by the transmembrane segment and also that the N-MBD interacts with the rest of the transporter in a metal ion-specific manner (Hou, 2001).

Immobilized metal affinity chromatography (IMAC) analysis of the amino-terminal domain of WDP revealed its varying affinities for different metals to be as follows: Cu(II)>>Zn(II)>Ni(II)>Co(II) (DiDonato, 1997). The metal binding properties were further examined in the same study with a zinc blotting assay. The amino-terminal domain was found to bind Zn(II) and in competition with Zn only Cd(II), Au(III) and Hg(II) were able to reduce the quantity of Zn(II)-protein complex. In similar studies using Cu (II) and Cu (I) as the competitor much lower concentrations of copper were needed to decrease Zn(II) binding. Additionally when the concentration was increased above a 10 μM threshold Zn(II) binding reduced drastically, suggestive of a cooperative binding mechanism. Another study found that Zn bound to the N-terminal domain of WDP is ligated primarily to nitrogen atoms unlike the sulfur ligands of cysteine which are involved in copper coordination (DiDonato, 2002). Conformational changes occur in WDP both upon binding of zinc and copper, however these changes are significantly different for each metal causing a loss of secondary structure in zinc, suggesting a plausible structure-based mechanism of the N-terminal domain for the discrimination of different metal ions *in vivo* (DiDonato, 2002).

Copper Binding

Copper maximally binds both MNK and WDP with a stoichiometry of six metal ions per protein in the reduced Cu(I) form such that each MBD is coordinated with copper in a 1:1 fashion (Lutsenko, 1997; Cobine, 2000). For determination of the oxidation state of copper bound to MNK and WDP, the proteins were denatured and assayed with bicinchoninic acid (BCA), a Cu(I)-selective chelator. The BCA-based assay was performed in the presence and absence of a reducing agent, ascorbate. Addition of ascorbate did not significantly alter the absorbance obtained using the BCA-based assay indicating the copper released from the protein was already in a reduced state as Cu(I). Additionally the BCA-based assay was used to determine the quantity of copper-bound to protein; increased quantities of copper were bound with the presence of ascorbate in the growth media (Lutsenko, 1997).

Further examination of the oxidation state of copper complexed to WDP has been performed using XAS (x-ray absorption spectroscopy) analysis (DiDonato, 2000). EXAFS (extended x-ray absorption fine structure) data indicates that each copper atom is ligated via two sulfur atoms both with a Cu-S distance of 2.17Å. These results are similar to the Cu-S bond distance observed in MNK (Cobine, 2000; Ralle, 1998). The Cu-S of 2.17 Å is between distances observed for trigonal and linear Cu (I)-thiolate complexes suggesting that copper is coordinated by two cysteines in a distorted linear geometry. By contrast, the crystal structure of the copper chaperone Atox1 reveals Cu(I) ion is ligated to two separate Atox1 molecules in a distorted tetrahedral geometry with three Cu-S distances of 2.3 Å and a fourth of 2.4 Å suggesting that copper may be either 3- or 4-coordinate (Rosenzweig, 2001). The monomer of the copper chaperone Atox1 was recently determined to bind copper in a 2-coordinate manner as determined by the NMR solution structure

(Anastassopoulou, 2004). The NMR solution structure of Cu(I) bound MNK MBD2 determined the ligand donating cysteines residues of the MBD were situated between the first β strand and the first α helix, a location close to the protein surface in a solvent accessible manner, and the S-Cu-S bond angle formed was $140^{o} \pm 40^{o}$ (Banci, 2004). Through comparison with the apo form of MNK MBD2 the cysteine containing loop was observed to undergo the most structural changes upon copper binding. The structure of MNK MBD2 is similar to other MBD structures of P-type ATPases and some copper chaperones, specifically the first MBD of the yeast homologue Ccc2 (Banci, 2001), Atx1 (an Atox1 yeast homologue) (Arnesano, 2001a) and MNK MBD4 (Gitschier, 1998).

XANES spectra of WDP showed a conserved peak at 8983 eV with varying stoichiometric concentrations of copper to protein (DiDonato, 2000). This peak is consistent with the $1s \rightarrow 4p$ transition of a Cu(I) center (DiDonato, 2000) as confirmed in the Cu(I)-thiolate model complexes $[Cu(SC_{10}H_{13})_2]^-$ and $[Cu(SC_6H_5)_3]^-$. This data clearly demonstrates that Cu bound to WDP is in the +1 oxidation state, and also that the metal binding coordination of the individual MBDs are quite similar to each other. The intensity of the transition at 8983 eV, which is indicative of the geometry around the Cu atom, is weaker than that of linear Cu-thiolate complexes, but stronger than that of trigonal compounds.

CD spectroscopy studies show progressive changes in the secondary and tertiary structure of WDP as the copper concentration is elevated (DiDonato, 2000). Secondary structure changes are evident in the increasingly negative molar ellipticity values measured at 208 nm and 222 nm indicative of an increase in helicity as copper is added to the protein. For the tertiary structure the aromatic region displays changes in magnitude and a loss of ellipticity at 330 nm, representing a loss of disulfide

bonds, as copper concentration increases. The combined CD and XAS data implicate that the binding environments surrounding the copper atoms remain unchanged during successive binding of copper while structural changes occur in the protein.

The rat homologue of WDP, designated rCBD, shares 80% homology with WDP yet contains only five repeats of the metal binding motif CXXC with the fourth MBD relative to WDP absent (Tsay, 2004). Recently, through structural homology modeling, the fourth MBD was identified within rCBD and showed the conserved βαββαβ fold characteristic of the MBDS (Tsay, 2004). Zn blotting assays reveal rCBD performs cooperative copper binding and metal ion discrimination similar to WDP. Comparisons of CD data for rCBD and WDP show the two proteins both undergo similar conformational changes upon addition of copper. Interestingly, the cooperative copper binding behavior of rCBD seems to be quite comparable to that of WDP despite the absence of one CXXC motif in the fourth "metal binding domain" signifying the importance of the βαββαβ fold in this metal binding and the subsequent conformational changes of the protein. The CXXC motif does appear to be necessary for Cu(I) coordination however since rCBD was capable of binding only five equivalents of copper (Tsay, 2004).

Binding Affinities and Copper Exchange

Recent studies have examined the MBDs of WDP regarding their affinity for Cu(I) (Wernimont, 2004). Although all six MBDs of WDP have been shown to be capable of binding copper (DiDonato, 1997), if different affinities for copper existed between the domains this would affect their roles in copper transport and copper-mediated events such as protein trafficking. Isothermal titration calorimetry (ITC) was used to measure the association constants (K_a) and stoichiometry (n) of Cu(I)

binding to the WDP MBDs (Wernimont, 2004). The association constants for all the MBDs and Atox1 were reported to be ~10^5-10^6 M^{-1} determining that the copper affinities of the MBDs are not responsible for their nonequivalent functionalities. However, the same study reported a higher binding affinity for the linked multi-domain protein MBD1-4 over the individual MBDs. These results indicate the affinity of the MBDs for copper may be influenced by the presence of other MBDs. The multi-domain product MBD1-6 was found to have an affinity for copper similar to the individual MBDs and Atox1 (Wernimont, 2004).

Copper exchange studies between the yeast proteins Ctr1 and Ccc2 as well as Ccc2 and Atx1 have provided insight into the mechanism of copper transfer by the MBDs and interacting proteins (Xiao, 2004; Huffman, 2000). The transfer of copper between the first MBD of Ccc2 (Ccc2a) and Atx1 has been examined using NMR titrations (Arnesano, 2001b). By monitoring the titrations of ^{15}N-labeled Cu(I)-Atx1 with the apo-Ccc2a MBD and ^{15}N-labeled Cu(I)-Ccc2a MBD with apo-Atx1 Arnesano et al. determined the two proteins were interacting and forming a transient protein-protein complex. The NMR data showed single signals for each labeled protein nucleus during the titrations. The chemical shift changes detected during the titrations were found to be dependent upon the quantity of unlabeled protein titrated. Furthermore, the apo and metal bound forms of the proteins exhibited distinct NH chemical changes between the free and complex states. Arnesano et al. concluded these results were consistent with a rapid exchange occurring between the free protein and protein-protein complex states. A mechanism for Cu(I) transfer between Atx1 and Ccc2a was proposed based upon the x-ray crystal structures of the proteins and NMR titration data. The mechanism is depicted in Figure 5. Copper exchange is mediated through the positioning of the two proteins by electrostatic forces. Next

Cys^{15} of Cu-Atx1, the most solvent exposed copper ligand, interacts with Ccc2a forming a protein-protein complex. As a result of complex formation Cys^{18} undergoes a conformational change. While the protein-protein complex is formed copper is quickly partitioned between the two proteins forming 2- and 3-coordinate intermediates with the proteins. The observed conformational changes between apo and Cu(I) bound states were greater for apo Atx1 than apo Ccc2a with the significant shifts occurring in loops 1 and 5 and helices α1 and α2. These regions are the nearest to the metal-binding site with loop 1 containing the metal-binding motif GMTCXXC. The mobility of apo Atx1 in these regions could favor dissociation of the chaperone from the complex.

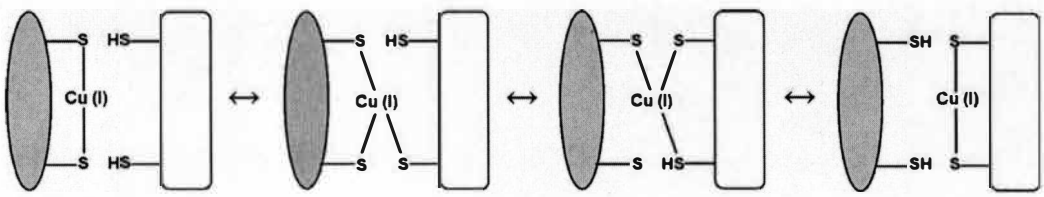

Figure 5. Proposed Mechanism for Cu(I) Exchange Between Atx1 and Ccc2a Using Ligand Exchange Reactions

Additionally the copper exchange between Atx1 and Ccc2a was studied in regards to understanding whether the reaction occurred under kinetic or thermodynamic control (Huffman, 2000). Similar to the findings by NMR titration the copper exchange was determined to reach equilibrium quite rapidly. Kinetic control of the reaction was suggested since only a small thermodynamic gradient was observed upon copper exchange between Atx1 and Ccc2, ~0.2 kcal/mol ($K_{exchange}$ = 1.4 ± 0.2). Upon consideration of the quantity of free copper within the cell,

estimated at less than 10^{-18}M (Rae, 1999), and the associated high capacity for copper chelation, one proposed mechanism for chaperone to maintain its specificity is via a slow kinetic rate constant, k_{off}, allowing the chaperone to retain copper despite the cellular environment (Wernimont, 2004). The complexation event between the chaperone and donor could alter k_{off}, reducing the kinetic activation barrier, and allowing copper exchange to occur. Recently another study involving copper exchange investigated dissociation constants of Cu(I) binding for the yeast proteins Ctr1, Ccc2, and Atx1. The experiments were conducted using the copper binding competitor bathocuproine disulfonate (BCS). BCS forms a stable copper complex with a known absorption coefficient and an overall association constant of $10^{19.8}$ for the species $Cu^{I}(bcs)_2^{3-}$ (Xiao, 2004). The change in absorbance was measured as copper was transferred from BCS to the protein of interest. The dissociation constants were estimated to be $\sim 10^{19}$ M, demonstrating the ability of these proteins to acquire copper under limiting conditions (Xiao,2004).

Significance of This Study

Few of the MBDs of either MNK or WDP have been independently expressed, purified, and characterized. Within WDP, three missence mutations of the N-terminal MBDs are known which result in Wilson disease, G85V (MBD1), L492S (MBD5), and G591D (MBD6). Comparison of the G85V mutant and wild type MBD1 could provide significant insight how a glycine → valine mutation within a single domain produces the disease state.

The similarity in secondary structure between the MBDs of MNK and WDP and the copper chaperone Atox1 in combination with the differences in electrostatic surface properties of these domains indicates a potential for domain-domain

interactions to occur. If present, these domain-domain interactions within the amino-terminal of the ATPase would represent an unexplored avenue of protein regulation. The fourth metal-binding domain of WDP was selected as a potential candidate for copper transfer with MBD1. The reasoning for this selection was based upon the predicted isoelectric points for the two domains being several pH units apart as MBD4 is considered the most acidic of the six MBDs.

Objectives of This Study

The goal of this study was to characterize domains one and four of the N-terminal metal binding domain of WDP and the disease-causing missence mutation of domain one, G85V. The domains were each cloned into an *E. coli* expression system, produced, and purified. The purified proteins, MBD1 and MBD4, were each characterized through means of high resolution gel filtration, MALDI mass spectrometry, and isoelectric focusing. Furthermore the abilities of each individual domain to bind copper and reversibly transfer the metal to the other domain were investigated. The copper exchange studies were performed at near physiological concentrations of copper in the range of 8-20μM within an anaerobic environment. The affect of varying molar ratios between the copper donor and acceptor was examined. The $K_{exchange}$ constant was calculated for the reaction. Separation of the proteins was achieved after copper exchange using strong anion exchange chromatography. The copper content of each protein after the exchange was determined using ICP-MS analysis.

CHAPTER II

MATERIALS AND METHODS

A plasmid containing the full-length human ATP7B gene was generously donated by Dr. Jonathon Gitlin of the University of Washington at St. Louis.

Cloning of WDP MBDs into *E. Coli* Expression Vectors

Primer design for metal-binding domains one and four of WDP was based upon the ATP7B gene sequence obtained from GenBank accession # U03464. MBD1 was amplified using forward primer 5′-CCT GGG CCC TTC TTC CAT GGT GGC CAC-3′ and reverse primer: 5′-AGA AGG ATA GGC AGG ATC CTG GCC CTC AAG-3′. Likewise MBD4 was generated using forward primer: 5′-CGA GAA ACC AGG CCA TGG GCA CAT GCA G-3′ and reverse primer: 5′-GTT TCC AAG AGG GAT CCT AGA ACA GCT TTC-3′. Primers were designed to incorporate an Nco I restriction site at the 5′-end and a BamH I restriction site at the 3′-end of the MBDs for directional cloning into expression vectors. The template DNA provided by Dr. J. Gitlin was used in the PCR reaction.

The PCR reactions each included the following: 5 μL DNA template (0.2 ng/μL), 0.6 μL Deep Vent DNA Polymerase (2 U/μL) from New England Biolabs, 5 μL of each forward and reverse primers (10 μM stock), 5 mL dNTP mix (2 mM stock), 5 μL 10x reaction buffer, and 24.4 μL reverse osmosis H_2O. Each PCR reaction was covered with 30 μL of mineral oil. For MBD1 the thermal cycling conditions were as following: one cycle of (a) 100°C for 5 minutes, (b) 63°C for 1 minute, (c) 72°C for 30 seconds, followed by twenty-nine cycles of (a) 100°C for 1 minute, (b) 63°C for 1 minute, (c) 72°C for 30 seconds. For MBD4 the thermal

cycling conditions were the same as those detailed for MBD1, with the exception of the temperature setting of step (b) being 57°C as opposed to 63°C for each cycle. The PCR products were verified by 1.8% agarose gel.

The MBD PCR products and the ampicillin resistant plasmid vector pET-21d (Novagen) were each digested with BamHI and NcoI (6 enzyme units each) for 4 hours at 37°C. Following digestion both the MBD PCR products and plasmid digests were purified using QIAquick PCR Purification Kit (Qiagen). After purification ligation reactions were constructed for insertion of the MBD genes into the plasmid vectors. For each MBD, three ligation reactions were prepared with varying molar ratios of MBD to plasmid vector (1:3, 1:1, and 3:1). Each 20 μL ligation reaction consisted of 200 ng plasmid, 2 μL 10x reaction buffer, 0.4 μL T4 DNA ligase (400 units/μL), varying concentrations of domains one or four, and reverse osmosis H_2O for final volume adjustment.

Each ligation reaction was incubated at 18°C for 4 hours and then transformed as detailed into competent *E. coli* DH5α cells. A 200 μL aliquot of competent cells was thawed on ice. 3 μL DMSO were added to the cells, mixed gently, and then the cells were incubated on ice for 30 minutes. The cells were heat shocked for 2 minutes at 42°C then incubated on ice for 2 minutes. Next 1 mL Luria Bertani (LB) media was added and the reaction was incubated at 37°C for 1 hour shaking at 250 rpm. The transformed DH5α cells were subsequently grown on LB agar media containing 100 μg/mL of the antibiotic ampicillin for 16-20 hours at 37°C

Colonies of DH5α cells were screened for the presence of recombinant plasmid using restrictive digestion analysis with the endonucleases BglII and BamHI. Colonies were first inoculated into 5 mL of LB and incubated at 37°C with shaking at 250 rpm overnight. The plasmids were isolated from bacterial culture using QIAprep

Mini Spin Kit and then digested with Bgl II and BamH I at 37°C for 4 hours to verify the ligation success. Once verified by restrictive digestion the recombinant plasmids were submitted for sequence analysis to Dr. Todd Barkman's lab, of the Biology Department at Western Michigan University.

Mutagenesis of Domain One

The mutated domain one was prepared using Stratagene's Quikchange XL site-directed mutagenesis kit. Mutagenic primers were designed to incorporate the G85V mutation. The sequence of the forward primer was: 5′ - GGA TTT CCA ATT TGA AAG TCA TCA ACA GCA TGA AGG TTT CC-3′ and the reverse primer sequence was: 5′-GGA AAC CTT CAT GCT GTT GAT GAC TTT CAA ATT GGA AAT CC-3′. The mutated domain was amplified using PCR. The PCR mixture included 5 μL of 10x reaction buffer, 1 μL dNTP mix, 3 μL Quik solution, 5 μL each of forward and reverse primer (2 μM), 0.35 μL of template plasmid (10 ng), and 30.7 μL of reverse osmosis H_20. After addition of 1 μL of pFu Turbo DNA polymerase the reaction was covered with 30 μL of mineral oil. The PCR thermal cycling parameters consisted of 1 min at 95°C, followed by 18 cycles of : 95°C for 50 seconds, 60°C for 50 seconds, 68°C for 7 minutes. After 18 cycles were completed the reaction was stored at 4°C. The parental DNA of the PCR reaction was selectively digested with 1 μL DpnI (10 u/μl) at 37°C for 60 minutes.

The mutated plasmid was then transformed into XL-10 Ultracompetent cells. A 45 μL aliquot of cells was thawed on ice. Next 2 μL β-mercaptoethanol were added to the cells, mixed gently, and then the cells were incubated on ice for 10 minutes. Once the mineral oil layer was removed 2 μL of DpnI digest were added to the cells. The transformation reaction was mixed gently and incubated on ice for 30 minutes.

The cells were heat shocked for 30 seconds at 42°C then incubated on ice for 2 minutes. Next 500 μL pre-warmed LB media were added and the reaction was incubated at 37°C for 1 hour shaking 250 rpm. The cells were plated onto LB agar plates containing 100 μg/mL ampicillin and incubated inverted overnight at 37°C. Colonies from the XL-10 transformation were inoculated into 5 mL cultures of LB media containing 100 μg/mL ampicillin and incubated at 37°C overnight shaking at 250 rpm. The plasmids were isolated from bacterial culture using QIAprep Mini Spin Kit. The isolated plasmid was run on a 1.2% agarose gel to determine the concentration and then submitted for sequence analysis.

Protein Expression Optimization

Prior to large scale protein production using 10 L cultures, time-course induction experiments were performed in 5 mL volumes to determine optimum conditions. Initially proteins were expressed in the *E. coli* strain BL21 (DE3) through the addition of the inducing agent isopropyl-1-thio-β-D-galactopyranoside (IPTG). A single colony of BL21(DE3) cells containing the recombinant plasmid was inoculated into 5 mL LB with 100 μg/mL ampicillin and incubated at 250 rpm, 37°C until the optical density at 600 nm (OD_{600}) was approximately 0.600 (0.45-0.65). A 500 μL background level aliquot was then collected, the OD_{600} recorded, and finally centrifuged for 2 minutes. The cellular pellet was stored at -20°C until ready for SDS-PAGE analysis. Upon reaching the desired OD_{600} value, protein expression was induced with the introduction of 1.0 mM IPTG into the growth media. The induced bacterial culture was incubated at 250 rpm, 37 °C for up to four hours. During this incubation 500 μL aliquots were collected every 30-60 minutes; each collected sample was treated as previously described for the background aliquot. Efficiency of

the protein expression was monitored by SDS-PAGE using 15% polyacrylamide 1 M Tris gels where the loading volumes for each aliquot were normalized against the background aliquot of 500 μL culture collected prior to IPTG induction.

Optimization studies of protein overexpression were performed by varying several factors including cell growth conditions, *E. coli* expression hosts, and induction parameters. To decrease loss of protein expression due to the possibility of a toxic eukaryotic gene product being encoded in an *E. coli* host, the Toxic Gene Induction protocol from Novagen was followed. Both the wild type and the G85V mutant of MBD1 were evaluated.

A single colony was inoculated into 2 mL Terrific Broth (TB) media containing 200 μg/mL carbenicillin and incubated at 37°C, 250 rpm until $OD_{600} \sim 0.4$. The cells were collected by centrifugation for 30 seconds, the supernatant removed, and the pellet resuspended in 2 mL fresh TB media. Next, 100 μl of resuspension was added to 8 mL TB media containing 500 μg/mL carbenicillin and incubated at 37°C until $OD_{600} \sim 0.4$. A 500 μL aliquot was collected as the background sample, and the pellet was stored at –20°C. The cells were collected by centrifugation at 1000 x g for 5 minutes and resuspended in 5 mL fresh TB media containing 500 μg/mL with 1 mM IPTG and incubated for 2 hours at 37°C, 250 rpm. An aliquot was collect in the same manner as the background sample after 2 hours. The samples collected were run on 15% Tris SDS-PAGE for analysis.

The effect of incubation temperature on the protein expression was studied both at 30°C and 37°C. Studies were conducted in two different ways. The first set of studies altered the temperature only after the addition of IPTG and onset of target protein expression and the initial incubation temperatures after inoculation were kept at 37°C. The second set of studies were conducted at a single temperature, either

30°C or 37°C, from inoculation until completion of the experiment. Temperature variance expression studies were conducted in LB and TB media. Attempts at examining expression in minimal media were not completed as > 12 hours were required to meet the necessary OD_{600} (0.45-0.65) for induction.

The effect of growth media on protein expression levels was also examined. MBD1 wild type, MBD1 G85V mutant, and MBD4 were each expressed in LB, TB, and minimal bacterial culture media. Each study included inoculating colonies into 5 mL of media containing 100μg/mL ampicillin and incubating until the cells' OD_{600} was within 0.45-0.65. At this point a 500 μL aliquot was collected, with recorded OD_{600}, and centrifuged for 2 minutes. The pellet was stored at -20°C until ready for SDS-PAGE analysis. The remaining culture was induced with 1mM IPTG and incubated for 2-4 hours at 37°C with 250 rpm shaking. Every 30 minutes an aliquot was collected, OD measured, centrifuged, and stored at -20°C. Again SDS-PAGE analysis was used to determine protein expression levels. The growth media experiments were also conducted with 1% glucose supplementation.

In addition to testing multiple media for optimization of protein expression, the use of rare codons in the protein nucleotide sequence was examined. Rosetta (DE3) cells (Novagen), derived from the BL21(DE3) *E. coli* strain, contain the genes to encode for several t-RNAs which are least abundant in *E. coli* yet commonly present in eukaryotic genes: AUA, AGG, AGA, CUA, CCC, and GGA. The recombinant plasmids containing the cloned MBDs were each transformed into competent Rosetta (DE3) cells. 20 μL aliquots of cells were thawed on ice for 5 minutes. 10 ng of plasmid DNA was added to the cells and incubated on ice for 5 minutes. The cells were heat shocked at 42°C for 30 seconds and then incubated on ice for 2 minutes. 80 μL of SOC media was added to the transformation reaction and

the tubes were incubated at 37°C with 250 rpm shaking for 1 hour. The reaction was subsequently plated onto LB agar plates containing 100 μg/mL ampicillin and incubated inverted at 37°C overnight. Expression studies previously conducted using LB, TB, and minimal media were each repeated in combination with altering the incubation temperature, using the Rosetta cells as the *E. coli* host.

The initial plasmid vector, pET-21d (Novagen), selected for cloning of the MBDs was an ampicillin resistant T7 RNA polymerase based plasmid. The genes for MBD1 wild type, MBD1 G85V mutant, and MBD4 were each cloned into the plasmid vector pET-24d (Novagen) which is different from the previous vector pET-21d only in its antibiotic resistance to kanamycin rather than ampicillin. Individual recombinant pET-21d plasmids containing MBD1, MBD1 G85V mutant, or MBD4 were digested with Nco I and BamH I at 37°C for 4 hours. The excised genes for the MBDs were purified from the digest using the QIAquick Gel Extraction Kit (Qiagen) after digest reactions were run on a 1.8% TBE agarose gel. pET-24d was also digested with the enzymes Nco I and BamH I under the same conditions. The plasmid digest was purified with the QIAquick PCR Purification Kit and subsequently ligated with the isolated MBD gene inserts. Conditions of the ligation reactions were the same as previously used when cloning the genes into pET-21d. The recombinant pET-24d plasmids were each transformed into Rosetta *E. coli* cells for further protein expression studies.

Lastly, optimization studies were conducted investigating the effects of IPTG concentration upon protein expression levels. Several experiments were performed on the recombinant pET-24d plasmid containing MBD1 using Rosetta cells as the *E. coli* expression host where IPTG concentrations ranged from 0.1 mM-2.0 mM. In addition to altering IPTG concentrations, the use of glucose supplementation,

different culture media, and incubation temperatures were also tested. Based upon results of MBD1 expression during these experiments MBD1 G85V and MBD4 expression levels were studied using LB and TB media at 30°C and 37°C using IPTG concentrations of 0.3 mM, 0.5 mM, 0.7 mM, and 1.0 mM.

Protein Expression and Purification

10 L Induction

A 10 L induction of both MBD1 and MBD4 was performed prior to purification of the proteins. A single colony was inoculated into 5 mL of LB media containing 30 μg/mL kanamycin and incubated at 37°C until OD_{600} reached 0.6. The cells were collected by centrifugation, 6000 rpm x 8 minutes using a Sorvall RC-5B+ centrifuge with SS-34 rotor. The cells were resuspended in 250 mL fresh LB media and 30 μg/mL kanamycin and incubated at 37°C until OD_{600} reached 0.6. The cells were collected by centrifugation, 6000 rpm x 8 minutes using a Sorvall RC-5B+ centrifuge with SLA-3000 rotor. The bacterial pellet was next resuspended in 10 L fresh LB media containing 30 μg/mL kanamycin. The culture was incubated at 37°C using a New Brunswick Microferm Fermentor with 500 rpm stirring and aeration of 10 psi until OD_{600} reached 0.6. An un-induced aliquot of 1 mL was collected for SDS-PAGE analysis. Protein overexpression was induced with addition of IPTG, final concentration, 0.5 mM. The cells were incubated at 37°C for 2 hours after IPTG induction, then harvested by centrifugation (6000 rpm x 8 minutes) in the same manner as before. Prior to centrifugation an induced aliquot of 1 mL was collected for SDS-PAGE analysis.

Freeze/Thaw Extraction of Protein

The bacterial cell pellets were frozen in liquid nitrogen for 10 minutes then thawed at room temperature for 40 minutes, this cycle was repeated two more times. The thawed pellet was resuspended in extraction buffer (20 mM MES/Na, 1 mM EDTA, 5 mM DTT, pH 6.0) using 24 ml buffer/ L cultured media. The suspension was gently shaken on ice for 1 hour. After incubation on ice the suspension was centrifuged for 15 minutes x 6000g at 4°C using a Sorvall RC-5B+ centrifuge with SLA-3000 rotor. The supernatant (containing protein) was collected for further purification. A 50 μL aliquot was collected for Bradford assay and SDS-PAGE analysis. The freeze thaw extraction treatment used selectively releases soluble cytoplasmic *E. coli* and recombinant proteins of less than 30 kDa in size through disruption of the outer cellular membrane and formation of pores within the cytoplasmic membrane (Johnson, 1994; Morris, 1993).

Batch Absorption Anion Exchange Chromatography

Crude MBD1 protein extract was first purified using a batch absorption anion exchange technique prior to loading the protein filtrate onto a cation exchange column. DEAE-Sepharose Fast-Flow resin (Amersham Pharmacia Biotech) was equilibrated in 20 mM MES/Na, 0.1 mM EDTA, 5 mM DTT, pH 5.5 by stirring gently for 30 minutes. The protein extraction was added to the resin and stirred for 30 minutes. The resin was allowed to settle and the supernatant was collected through a Buchner funnel using a Whatman #41 filter. A 50 μL aliquot of the MBD1-containing filtrate was collected for Bradford assay and SDS-PAGE analysis. The flow-through was then filtered with a 0.22μm filter before loading onto the FPLC for further purification. For removal of ionically-bound proteins, the DEAE resin

was resuspended in high salt buffer, 20 mM MES/Na, 0.1 mM EDTA, 5 mM DTT, 1 M NaCl, pH 5.5 and stirred for 30 minutes. The resin was allowed to settle and filtered through a Buchner funnel. An aliquot of the high salt filtrate was collected for Bradford assay and SDS-PAGE analysis.

Ion Exchange Chromatography Employing FPLC

An Amersham Pharmacia Biotech AKTA Design FPLC system was employed for all column chromatography techniques described hereafter. The FPLC system used is capable of monitoring the ultraviolet absorbance at 254 nm or 280 nm during sample fraction elution. Absorbance was selected to be monitored at 254 nm as the absorbance peaks were amplified over those measured at 280 nm due to the low quantity of aromatic residues present in either protein responsible for A_{280} (amino acid sequences are presented in Figure 3). CM-Sepharose Fast-Flow resin was employed for ion exchange purification of MBD1 whereas DEAE-Sepharose Fast-Flow resin was used for MBD4. Each chromatography column was packed with degassed resin at a rate of 2.5 mL/min to yield a total column volume of approximately 80 mL. Prior to protein loading each column was equilibrated with low salt buffer, (20 mM MES/Na, 0.1 mM EDTA, 5 mM DTT, pH 5.5) using four column volumes at a flow rate of 2.0 mL/min. The filtered protein samples were each loaded onto the columns at a flow rate of 2.0 mL/min. During sample loading the column flow-through was collected and labeled as Fraction A. The columns were then re-equilibrated with the low salt buffer for removal of any unbound protein using 2 column volumes of low salt buffer; the flow-through collected was labeled as Fraction B. A salt-gradient was next applied over three column volumes, increasing the salt concentration from initially 0% of high salt buffer (20 mM MES/Na, 0.1 mM

EDTA, 5 mM DTT, 1M NaCl, pH 5.5,) to a final concentration of 50%. The salt gradient eluants were collected in 3.3 mL fractions, 95 fractions were collected altogether. In conjunction with the UV absorbance recorded during the ion exchange Bradford assays were performed on every third fraction within to determine where the protein eluted. SDS-PAGE analysis was performed on fractions with higher Bradford readings. Samples with protein present were combined and concentrated to a volume of approximately 2.0 mL using a 60 mL Amicon Ultra-filtration cell.

Gel Filtration

Gel filtration was used to further purify the protein by size exclusion. Superdex 75 prep grade resin packed in a 26/60 column (Amersham Pharmacia Biotech) with an approximate column volume of 330 mL was used. After removal of the 20% ethanol storage solution using 2 column volumes reverse osmosis H_2O the column was equilibrated using a buffer containing 20 mM MES/Na, 10 mM DTT, 150 mM NaCl, pH 6.0. The protein-containing sample was loaded into a pre-washed syringe, and then injected into the 2.2 ml injection loop. Prior to sample injection the column was briefly re-equilibrated with 0.1 column volumes. Fractions of 5.1 mL were collected for 1.5 column volumes, 95 fractions were collected in total. Bradford assays were performed on every third fraction within the absorbance peak containing range to determine target protein containing eluants. SDS-PAGE analysis was performed for verification of Bradford assay results.

Protein Quantification

Several methods were employed to verify the purity, mass, and concentration of the purified proteins. Amino acid hydrolysis was performed on both MBDs by the

Texas A&M University Protein Chemistry Laboratory for determination of protein amino acid composition and furthermore for quantification of the molar concentrations for each protein solution. Matrix Assisted Laser Desorption Ionization time-of-flight (MALDI TOF) mass spectrometry was also utilized as a means to verify purity as well as determine the molecular mass of the isolated proteins. Based upon the amino acid hydrolysis established protein concentrations, a Bradford assay (Bio-Rad) standard curve was constructed for each protein. The Bradford assay is based upon the shift in absorbance that occurs when Coomassie Brilliant Blue binds to the arginine and aromatic residues of proteins in solution causing the dye to turn from a red to blue color (Bradford; 1976); the absorbance is measured at 595 nm for the assay.

Additionally protein concentrations were determined by using a Thiol and Sulfide Quantitation Kit (Molecular Probes). The concentration of thiols in each protein can be attributed to the cysteines residues, of which 4 are present in MBD1 and 3 in MBD4. The method employed for thiol quantitation was a modified Ellman's assay utilizing the enzyme papain for increased sensitivity. Ellman's assay is a spectrophotometric method for determining thiol concentrations (Ellman, 1959). The assay is based upon the reaction of Ellman's reagent [5,5′-dithiobis(2-nitrobenzoic acid), DTNB] to form a disulfide bond with the thiols of the sample. The stoichiometric formation of the yellow colored product, TNB thiolate (5-thio-2-nitrobenzoate, TNB^-), can be measured at 412 nm. The thiol concentration of the sample can calculated using Beers Law and the extinction coefficient of TNB^-. The reactivation of the enzyme papain by thiols provides an assay with a 100-fold increased sensitivity for thiols over Ellman's assay (Singh, 1993). The reactivated papain is quantitated by its enzymatic activity with the substrate N-benzoyl-L-

arginine-p-nitroanilide; the amount of chromogenic p-nitroaniline generated through enzymatic cleavage of the substrate can be measured by absorbance at 410 nm.

Isoelectric Focusing

The isoelectric focusing of all the purified MBDs of WDP recently produced (MBD1, MBD3, MBD4, MBD6, and MBD5-6) in the laboratory of Dr. David Huffman was accomplished using pH 3-9 gradient gels maintained at 15°C on a Pharmacia PhastSystem separation unit. The IEF program consisted of three steps: pre-focusing, sample application, and focusing. The programmed parameters for each step are detailed as follows: pre-focusing at 2000 V, 2.5 mA, 3.5 W for 75 volt hours, sample application at 200 V, 2.5 mA, 3.5 W for 15 volt hours, and focusing at 2000 V, 2.5 mA, 3.5 W for 410 volt hours. For each protein approximately 1 μg was used for analysis. For isoelectric point determination the Broad Range pI Calibration Kit from Amersham Pharmacia Biotech was used. Staining of the IEF gels was performed manually and consisted of four steps: (a) fixing the gel at room temperature for 10 min. with 20% trichloroacetic acid, (b) rinsing at room temperature for 2 min. using a 10% acetic acid, 30% methanol solution, (c) staining at 50°C for 20 min. with a 0.02% Coomassie Brilliant Blue, 0.1% copper(II)sulfate, 10% acetic acid, 30% methanol solution, and (d) destaining at 50°C for 30 min. with a 10% acetic acid, 30% methanol solution.

High Resolution Gel Filtration

High resolution gel filtration was used to broadly characterize the proteins for molecular mass properties. Two columns, Superdex 75 10/30 HR and Superdex Peptide HR 10/30 (Amersham Pharmacia Biotech), were employed to provide a

better estimate of protein mass. The Superdex 10/30 HR column was calibrated with the following molecular mass standards: ovalbumin (43,000 Da), chymotrypsinogen A (25,000 Da), ribonuclease A (13,700), and bovine serum albumin (7,000 Da). The column void volume was determined using blue dextran. Purified proteins of MBD1, MBD5, and MBD5-6 of WDP were each loaded onto the Superdex 10/30 HR column and eluted with 20 mM MES/Na, 10 mM DTT, 150 mM NaCl, pH 6.0 at a flow rate of 0.5 mL/min. Collected fractions of 0.5 mL were analyzed for protein content using SDS-PAGE. For molecular mass calibration of the Superdex Peptide 10/30 HR column the following standards were used: myoglobin (17,800 Da), ribonuclease A (13, 700 Da), cytochrome c (12,500 Da), aprotinin (6,500 Da), gastrin I (2,126 Da), vitamin B_{12} (1,355 Da), $(glycine)_6$ (360 Da), $(glycine)_3$ (189 Da), and glycine (75 Da). As before, blue dextran was used to calculate the column void volume. Proteins of metal-binding domains 1, 4, 6, and 5-6 were each loaded onto the Superdex Peptide 10/30 HR column. Each protein was eluted from the column with 20 mM phosphate, 150 mM NaCl, 10 mM DTT, pH 7.1 at a flow rate of 0.5 mL/min. Additionally experiments were repeated with the more acidic proteins, domains 4 and 6, where the elution buffer was changed to 20 mM Tris/Cl, 150 mM NaCl, 10 mM DTT, pH 8.0 to examine pH effects on the gel filtration molecular mass determinants.

Copper Binding and Interdomain Copper Exchange

All handling of proteins during the metal binding and copper exchange studies was carried out in an N_2 atmosphere chamber maintained at 18°C (Nexus Standard Glove Box System, Vacuum Atmospheres Co.). Buffers were treated with Chelex-100 resin to minimize the background level of copper present during the studies. The

metal binding and copper exchange events were performed in a single buffer: 20 mM MES/Na, 150 mM NaCl, pH 6.0. Copper binding was accomplished in a 10 ml Amicon Ultra filtration cell fitted with an YM3 Millipore membrane, molecular weight limit of 3,000 Da. For preparation of Cu-MBD1 and Cu-MBD4 1.0 molar equivalent of $Cu^{(I)}(CH_3CN)_4]PF_6$ was added to each MBD to give a final protein concentration of 30 μM in 7 mL. The Cu(I)-protein solution was stirred for 10 minutes before exchanging the buffer four consecutive times to remove any unbound copper. Each flow-through fraction collected during the buffer exchange was saved for later copper analysis.

The $[Cu^{(I)}(CH_3CN)_4]PF_6$ stock solution was prepared by dissolving the metal compound in a 2% acetonitrile matrix. The Cu(I) concentration of the stock solution was determined via a Thermo Elemental VG PQ Excell ICP-MS (Northwestern University). A trace metal grade Cu standard was used for calibration of the Cu(I) stock solution concentration. Two copper calibrations were performed; the first calibration range included 0 ppb – 100 ppb Cu and the second calibration range included 0 ppb – 10 ppb Cu. The second calibration was used for determination of the background copper. The mean of three ICP-MS instrumental readings was used for all calculations of copper quantities.

Copper exchange between MBD1 and MBD4 was executed through the mixing of (a) Cu-MBD1 with apo MBD4 for the forward reaction or (b) Cu-MBD4 with apo MBD1 for the reverse reaction, in an inert environment with 5 minutes of incubation at 18°C. Afterward the solution was immediately loaded onto a 1 mL HiTrap Q-Sepharose HP column (Amersham Pharmacia Biosciences) for separation of the two MBDs using a linear salt gradient increasing from 150 mM NaCl to 400

mM NaCl. Collected column fractions were analyzed in terms of protein concentration and metal content using the Bio-Rad assay and ICP-MS, respectively.

The copper exchange experiments were each done with three separate molar ratios of Cu-MBD to apo MBD (1:1, 2:1, and 1:2). Copper exchange reactions were done in a 1.2 mL volume using 1.5 mL Eppendorf tubes with protein concentrations ranging from 10 μM to 20 μM.

CHAPTER III

RESULTS

Cloning of WDP MBDs

The genes for MBD1 and MBD4 were each amplified through 30 cycles of PCR using Deep Vent DNA Polymerase (New England Biolabs). PCR products of the MBDs double digested with the endonucleases NcoI and BamHI and purified before directionally cloning the genes the *E. coli* expression vector pET-21d. Sequence analysis was performed on the recombinant plasmids containing MBD1 and MBD4 before commencing to synthesize protein. The sequence for each cloned MBD is provided in Figure 6; the sequences in Figure 6 are aligned to by the conserved metal-binding motif GMCXXC. The MBD1 G85V mutant was generated using Stratagene's Quikchange XL site-directed mutagenesis kit. MBD1 wild type and mutant forms are both 72 amino acid residues in length with the mutation occurring as the second most N-terminal glycine residue. MBD4 is 75 amino acids in length and shares 47% sequence identity with MBD1.

Protein Expression in *E. coli*

Initially each MBD was individually cloned into the pET- 21d expression vector and transformed into BL21 (DE3) *E. coli* hosts. For protein expression, plasmid-containing cells were inoculated into LB with the appropriate antibiotic (ampicillin in the case of plasmid pET-21d) and incubated at 37°C until the desired OD_{600} was reached, at which point protein expression was induced with 1 mM IPTG. Figure 7 shows a 15% SDS-PAGE of a time-course study of MBD1 protein

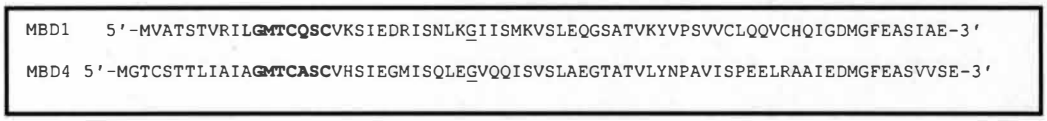

Figure 6. MBD1 and MBD4 Amino Acid Sequences

Each MBD sequence shares the conserved GMTCXXC motif, outlined in bold, and is approximately 70 amino acid residues in length. The mutant of MBD1 contains a missence mutation where a conserved glycine, underlined above, is changed to valine.

expression; the protein samples have been normalized against a background sample (time = 0 min.) for determination of target protein overexpression. After examining the results of the expression studies of MBD1 wild type, the protein was considered to be poorly overexpressing under the given experimental conditions. Several parameters of the protein expression protocol were changed to optimize the protein yield.

One possible cause for the poor overexpression of MBD1 is the presence of rare amino acid codons in the protein sequence (Novagen, 2003). Some eukaryotic proteins contain codons seldom used in *E. coli*. When overexpression is induced the low t-RNA levels of these rare codons can adversely affect the protein expression levels. MBD1 was found to contain one such rare codon, AUA, for its most N-terminal alanine residue. Rosetta *E. coli* cells (Novagen) contain t-RNAs for six codons that are rarely used in *E. coli*, including the AUA codon present in MBD1. For prevention of low protein yields due to rare codon usage each MBD studied was transformed into Rosetta cells for future studies.

The MBDs were each studied for protein expression levels when using different growth media: LB, TB, and M9 minimal. While growth media did influence rates at which inoculated cultures reached the desired OD_{600} for induction, protein

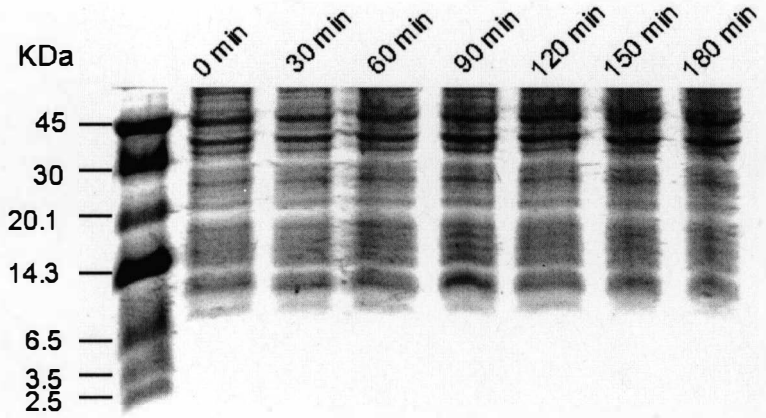

Figure 7. Initial MBDl Time-course Expression Studies Exhibit Low Protein Yields

Experimental conditions: BL21 (DE3) as the *E. coli* expression host, ampicillin resistant pET-21d expression vector, Luria broth for culture media, 37°C incubation temperature, and 1 mM IPTG for induction.

expression levels were not discernible between the different media. In order to determine whether basal expression levels of the target protein were masking the protein expression induction, media was supplemented with 1-2% glucose. pET-21d and pET-24d vectors each contain a T7 promoter sequence upstream of the target gene for selective transcription of plasmid DNA by T7 RNA polymerase. T7 RNA polymerase gene expression and transcription activity are regulated by the *lac*UV5 promoter located within the *E. coli* cellular DNA. The *lac*UV5 promoter is activated with the addition of the lactose analog IPTG to induce protein expression. However, the *lac*UV5 promoter may also be stimulated by cAMP causing an increase in basal expression levels of target protein. The addition of glucose to media helps prevent cAMP-triggered target protein expression (Baneyx, 1999). Protein expression studies conducted in glucose supplemented media showed no changes from non-supplemented media.

The antibiotic selectivity of the plasmid prevents overgrowth of the bacterial culture by cells which lack the vector plasmid (Novagen, 2003). As a bacterial culture proceeds from the logarithmic growth phase toward the saturation growth phase, fewer plasmid-containing cells endure. Initially the MBDs were cloned into pET-21d, an ampicillin resistant expression vector and yielded poor expression of target protein. MBD1 and MBD1 mutant were both expressed using the ampicillin analog carbenicillin which is less susceptible to the acidic pH changes that occur in the growth medium due to bacterial metabolic processes. Replacing ampicillin with carbenicillin did not increase protein yields.

In addition to carbenicillin and ampicillin, kanamycin was also used for antibiotic selection. Kanamycin is less susceptible to degradation than ampicillin. In addition, the pET- 24d vector produces less antibiotic gene product during induction than pET-21d. This is due to the location and orientation of the β-lactamase gene (responsible for ampicillin resistance) within pET-21d and the kan gene in pET-24d. In both plasmids the antibiotic gene is located downstream of the T7 promoter where mRNA synthesis is initiated. As a result, when the T7 promoter of pET-21d is induced, target protein mRNA is produced as well as some mRNA for the ampicillin resistant enzyme β-lactamase, resulting in an increase in antibiotic degradation after IPTG induction. This problem is corrected in the pET-24d vector by changing the orientation of the kan gene. Each MBD gene was shuttled from pET-21d to pET-24d to use kanamycin for antibiotic selection of the plasmid-containing cells. Protein expression studies conducted using pET-24d as the expression vector displayed an improvement over previous studies performed with pET-21d. A detectable band appeared on polyacrylamide gels of time-course protein expression studies which corresponded well to the expected target protein molecular mass (results not shown.)

Slowing the rate of protein synthesis can produce greater quantities of protein in an active and soluble form. Incubation temperature and IPTG concentration during protein expression were each examined with consideration of their effects on protein synthesis rates. Time-course protein expression studies show little difference between cultures incubated at 30°C and 37°C if the incubation was continued for at least 3 hours. Differences in OD_{600} readings of the induced cultures for each temperature during incubation periods of less than 3 hours can be contributed to the differences in growth rates for the two temperatures. IPTG concentrations from 0.1-2.0 mM were studied for MBD1 protein expression. At concentrations of 1 mM IPTG or greater MBD1 was poorly overexpressed in the *E. coli* cells. When the IPTG concentration was lowered to 0.7 mM or less MBD1 expression was readily detectable through SDS-PAGE analysis. The optimal concentration of IPTG for MBD1 expression was determined to be 0.5 mM. Figure 8 shows a 15% SDS-PAGE of a time-course study of MBD1 optimized protein expression with normalized loading volumes.

The G85V mutant of MBD1 and MBD4 expression levels were also optimized using the same parameters as described for MBD1. Successful expression of the MBD1 mutant was not achieved during this study. MBD4 was found to express well under the same conditions as MBD1: *E. coli* Rosetta cell expression host, kanamycin resistant pET-24d expression vector, Luria broth for culture media, 37°C incubation temperature, and 0.5 mM IPTG for induction. The expression of MBD4 was not readily detected by staining the polyacrylamide gels of MBD4 induction studies with Coomassie Brilliant Blue. However, overexpression of MBD4 was detected without difficulty using a silver staining kit (Amersham Biosciences). Both MBD1 and MBD4 were found to be expressed with >90% of the total protein

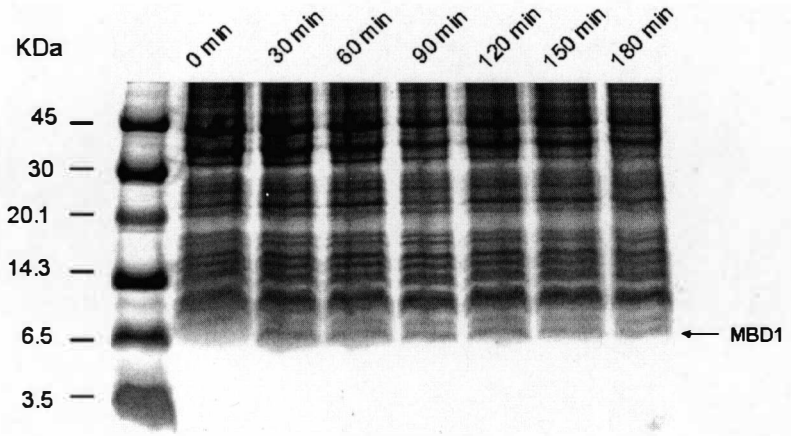

Figure 8. Optimized Yield for MBD1 Time-course Expression Studies

Experimental conditions: Rosetta cells as the *E. coli* expression host, kanamycin resistant pET-24d expression vector, Luria broth for culture media, 37°C incubation temperature, and 0.5 mM IPTG for induction.

yield present in a soluble form as determined by comparisons of polyacrylamide gels of the total cell extracts, the soluble protein isolated by freeze thaw extraction treatment, and the proteins remaining in the cellular pellet after freeze thaw treatment (results not shown).

Protein Purification

A large-scale overexpression was conducted for MBD1 and MBD4 using a 10 liter LB culture for induction. Each 10 L induction was performed using a New Brunswick Microferm Fermentor. Incubation conditions were set as 37°C with 500 rpm stirring, and 10 psi of aeration. The cultures were allowed to induce for 2 hours prior to being harvested. Bacterial cellular pellets were treated to a freeze thaw extraction to selectively release soluble proteins with a molecular mass of < 30 kDa

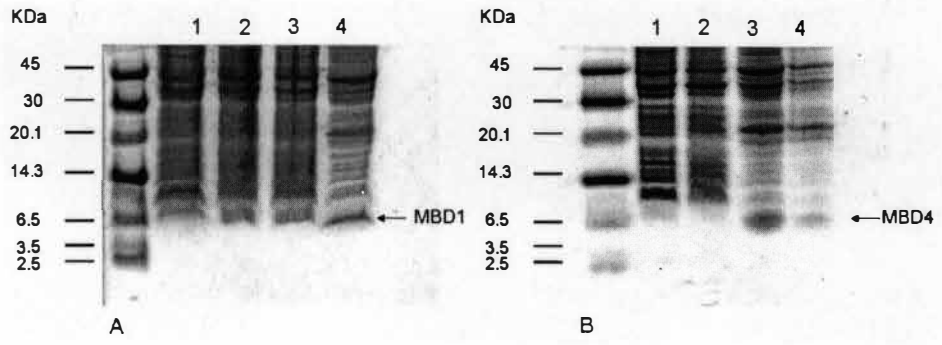

Figure 9. 10 L Overexpression of MBD1 and MBD4

15% Tris SDS-PAGE (A) MBD1 10 L induction. Loaded samples include (1) un-induced culture, (2) 1 hr induction aliquot, (3) 2 hr induction aliquot, and (4) freeze thaw extraction. (B) MBD4 10 L induction. Loaded samples include (1) un-induced culture, (2) 2 hr induction aliquot, (3) freeze thaw extraction precipitated with TCA, and (4) freeze thaw extraction.

(Johnson, 1994). The results of the large-scale overexpression and subsequent freeze thaw extraction treatment of MBD1 and MBD4 are shown in Figure 9. The MBD1 and MBD4 crude protein extracts were purified using separate weak ion exchange protocols.

Due to the acidic nature of most *E. coli* cellular proteins, having a pI typically less than 6, a batch DEAE-Sepharose anion exchange was performed on crude MBD1 extract to remove most cellular proteins. The batch anion exchange was buffered to pH 5.5. MBD1 has a theoretical pI value of 7.8 (Huffman, 2001) and therefore should not bind to the DEAE resin under acidic pH conditions. After batch anion exchange the protein was further purified by CM-Sepharose cation exchange using an AKTA FPLC system. The batch exchange technique was a preferred method over directly proceeding with ion exchange chromatography by FPLC in the purification of MBD1. The *E. coli* cellular proteins removed during this step bind strongly to the DEAE resin and require extensive cleaning of the resin prior to further use.

MBD4 has a theoretical pI value of 3.8 (Huffman, 2001) and therefore the use of a batch ion exchange technique for cleaning the crude protein extract, as was done with MBD1, would not be effective. Instead, crude MBD4 protein extract was directly purified by DEAE-Sepharose anion exchange under the same conditions as MBD1 ion exchange FPLC purification. Both proteins were purified using the same buffer, 20 mM MES/Na, 0.1 mM EDTA, 5 mM DTT, pH 5.5, with a 0-0.5 M NaCl salt gradient. FPLC fractions of 3.3 mL were collected during the salt gradient and analyzed for protein content. MBD1 was found to elute during fractions 45-63 with NaCl concentrations of 0.2-0.3 M with few impurities. MBD4 eluted during fractions 60-70 at 0.4-0.45 M NaCl along some cellular proteins. Figure 10 is an SDS-PAGE of the fractions collected during ion exchanges which contain the MBDs.

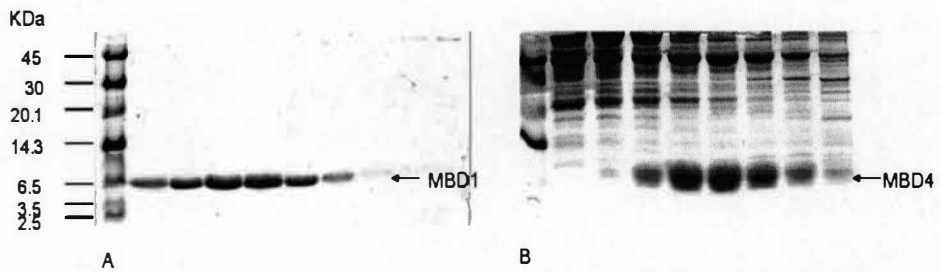

Figure 10. Ion Exchange Chromatography of MBD1 and MBD4

(A) Fractions 45, 48, 51, 54, 57, 60, and 63 of the CM-Sepharose cation exchange were determined to contain MBD1. (B) Fractions 60, 62, 64, 66, 68, and 70 of the DEAE-Sepharose anion exchange contained MBD4.

Protein-containing fractions from ion exchange chromatography were combined and concentrated using an Amicon Ultra-filtration cell until the volume was less than 2.5 mL. For the final purification step each protein solution was loaded onto a gel filtration column containing Superdex 75 prep grade resin and eluted with buffer (20 mM MES/Na, 10 mM DTT, 150 mM NaCl, pH 6.0). Fraction volumes of

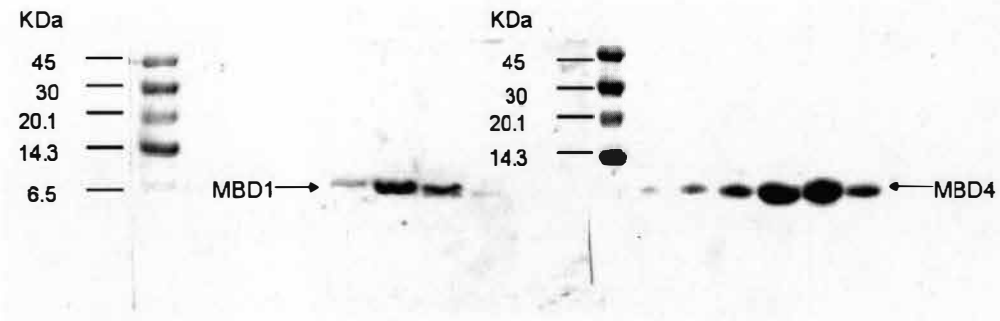

Figure 11. Purified MBDs 1 and 4

Superdex 75 gel filtration fractions containing MBD1 and MBD4 run on 15% Tris SDS-PAGE. The proteins are each considered to have been purified to homogeneity after gel filtration.

5.1 mL were collected and analyzed by Bio-Rad and SDS-PAGE. Protein-containing fractions collected during gel filtration for each domain are shown in Figure 11. MBD1 and MBD4 very similar in size and thus were both collected during fractions 39 to 45 for each respective isocratic elution.

Characterization of MBDs

The purified WDP MBDs were analyzed in terms of amino acid composition and molecular mass in order to verify proper protein identity and lack of contamination. Amino acid hydrolysis of MBD1, MBD4, and MBD6 were performed by the Texas A & M University Protein Chemistry Laboratory. The percent amino acid composition ascertained for each MBD agreed well with the known values. Amino acid hydrolysis was also used for calculation of protein concentration for each homogeneous protein sample and determination of protein yield from a 10 L induction. Approximately 4.5 mg of MBD1, 27.5 mg of MBD4, 20 mg of MBD6 were obtained per 10 L culture. The hydrolysis results were further

utilized for an external calibration of protein concentrations determined using the Bradford assay with an IgG standard. The Bradford assay underestimated the concentration of each protein studied; MBD1 was underestimated by 33%, MBD4 by 92%, and MBD6 by 65%. The Bradford assay underestimated with increasing amounts as the proteins became more acidic.

MALDI-TOF mass spectrometry data for MBD1 and MBD4, shown in Figure 12, were obtained through the Michigan State Mass Spectrometry Lab. The calculated average molecular masses of MBD1 and MBD4 are 7777 Da and 7720 Da, respectively. For MBD1 the largest peak is present at 7777.17 Da within the mass spectrum and no other substantial peaks are detected. The MBD4 mass spectrum shows two significant peaks at 7593.10 Da and 7724.74 Da. The larger mass, 7724.74 Da, is very close to the calculated mass of 7720 Da. The difference between the two peak values, 131.64 Da, is readily explained upon considering the occurrence of N-terminal methionine-processing.

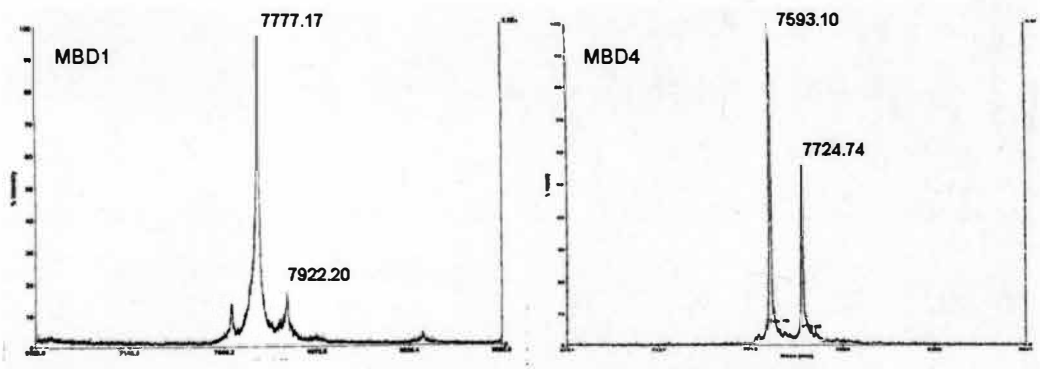

Figure 12. MALDI-TOF Data for MBD1 and MBD4

The MBDs of WDP have been predicted have to distinct surface potentials with pI values ranging from 3.8 (MBD4) to 8.7(MBD2) as detailed in Figure 3. MBD4 was chosen to study alongside MBD1 in part because of its significantly low pI value; MBD4 is the most acidic of the six N-terminal metal-binding domains. In addition to MBD1 and MBD4, other purified MBDs of WDP recently produced in the laboratory of Dr. David Huffman were also analyzed including: MBD3, MBD6, and the linked domains MBD5-6. Experimental determination of the pI values was performed using pH 3-9 gradient gels on a Pharmacia PhastSystem with the Broad Range pI Calibration Kit from Amersham Pharmacia Biotech. The calibration curve constructed from the pI standards was obtained by a linear least squares fit analysis of the data. Results of the isoelectric focusing are shown in Figure 13. As predicted by computer modeling (Huffman, 2001), the individual isolated domains 1, 3, 4, and 6 each have a unique isoelectric point. Notably, the determined pI values for MBD1 and MBD4 were almost 3 pH units apart.

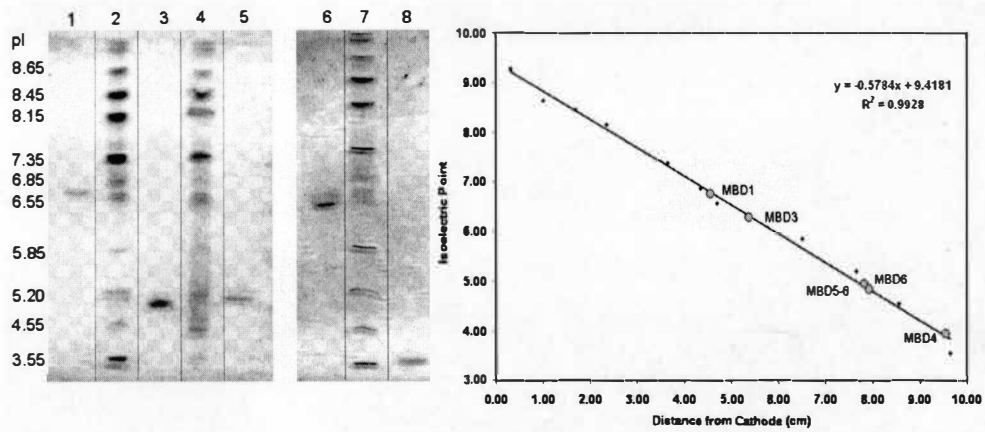

Figure 13. Isoelectric Focusing of WDP MBDs

Determination of the isoelectric points for the individual WDP domains: MBD1 pI = 6.77 (lane 1), MBD3 pI = 6.31 (lane 6), MBD4 pI = 3.85 (lane 8), MBD6 pI = 5.02 (lane 5), and MBD5-6 pI = 4.96 (lane 3). Isoelectric point protein standards (lanes 2, 4, and 7) were fit by least squares analysis for the calibration curve shown.

Each isolated protein (MBD1, MBD4, MBD6, and MBD5-6) was analyzed by high resolution gel filtration spectroscopy to verify sample purity and characterize the apparent molecular masses for the domains. Two columns, Superdex 10/30 HR and Superdex Peptide (Pharmacia Biosciences), were used for the high resolution gel filtration studies. A single Gaussian peak was observed for each protein sample analyzed by high resolution gel filtration indicating an apparent lack of protein aggregation. Figure 14 shows two gel filtration profiles which are representative of the entire gel filtration experiment sample set through the differences in experimental parameters. For each experiment UV absorbance was measured at 254 nm by FPLC. The gel filtration profile shown of MBD1 was conducted with MES buffer at pH 6.0 using the Superdex 10/30 HR column. The gel filtration profile of MBD4 was generated using phosphate buffer at pH 7.1 and the Superdex Peptide 10/30 HR column. Table 1 lists the molecular masses for the protein standards and MBDs with corresponding elution volumes for each column. Both columns produced an overestimate of molecular mass for the MBDs; the Peptide column showed some

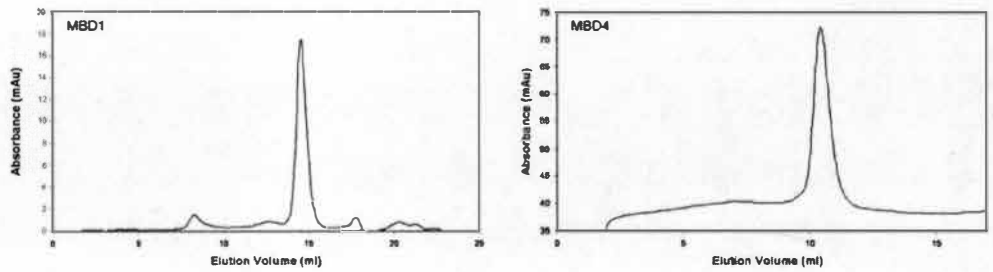

Figure 14. High Resolution Gel Filtration Profiles

For molecular mass estimation 137 μg of MBD1 was injected onto a Superdex 10/30 HR column (left); 390 μg of MBD4 was injected onto a Superdex Peptide 10/30 HR column (right).

Column:	Superdex 10/30 HR				Superdex Peptide 10/30 HR				
Protein Standards	**V_t (ml)**	**K_{av}**	**Mass (Da)**		**Protein Standards**	**V_t (ml)**	**K_{av}**	**Mass (Da)**	
Blue Dextran 2000	8.20		$> 10^6$		Blue Dextran 2000	8.12		$> 10^6$	
Bovine Serum Albumin	10.09	0.123	67,000		Myoglobin	9.82	0.110	17800	
Ovalbumin	10.95	0.179	43,000		Rnase A	10.08	0.127	13700	
Chymotrypsinogen A	13.06	0.316	25,000		Cytochrome C	10.17	0.133	12500	
Ribonuclease A	13.99	0.377	13,000		Aprotinin	11.69	0.231	6500	
					Gastrin I	14.05	0.384	2126	
					Vitamin B12	16.14	0.519	1355	
					Glycine 6	17.78	0.626	360	
					Glycine 3	18.79	0.691	189	
					Glycine	19.84	0.759	75	
Protein Unknowns	**V_t (ml)**	**K_{av}**	**Mass (Da)**	**Calc. Mass (Da)**	**Protein Unknowns**	**V_t (ml)**	**K_{av}**	**Mass (Da)**	**Calc. Mass (Da)**
Wilson Domain 1	14.530	0.412	7777	12,200	Wilson Domain 1	10.91	0.181	7777	9,700
Wilson Domain 6	14.360	0.401	7732	13,100	Wilson Domain 4	10.41	0.148	7720	12,600
Wilson Domain 5-6	12.650	0.290	15995	25,500	Wilson Domain 4'	10.46	0.152	7720	12,300
					Wilson Domain 6	10.85	0.177	7732	10,000
					Wilson Domain 6'	10.94	0.183	7732	9,600
					Wilson Domain 5-6	9.45	0.086	15995	20,600

Table 1. HR Gel Filtration Data for WDP MBDs

High resolution gel filtration of the MBDs was conducted with two separate columns: Superdex 10/30 HR and Superdex Peptide 10/30 HR. All separations performed with the Superdex 10/30 HR column used a 20 mM MES/Na, 10 mM DTT, 150 mM NaCl, pH 6.0 buffer. The Superdex Peptide 10/30 HR column was eluted with 20 mM phosphate, 150 mM NaCl, 10 mM DTT, pH 7.1 buffer for each protein characterization. MBD4 and MBD6 were also eluted from the Peptide column using 20 mM Tris/Cl, 150 mM NaCl, 10 mM DTT, pH 8.0; use of the Tris buffer is denoted by an asterisk.

improvement over the Superdex 10/30 HR column in determining mass. In addition, adjusting the elution buffer pH for the Peptide column was shown to affect the elution volume of the more acidic proteins, MBD4 and MBD6, and subsequent molecular mass calculation.

Copper Transfer

Currently, no studies of copper (I) exchange between individual MBDs of WDP have been published. Previous studies have all examined the copper binding

characteristics of the domains using from two to six of the MBDs either by mutating the cysteine residues of the metal binding site GMCXXC motif or by cloning methods. Preparation of the metallated proteins was performed in an N_2 atmosphere chamber maintained at 18°C (Vacuum Atmospheres). Initial control studies of the apo and Cu-loaded MBDs determined that successful separation of the proteins could be accomplished using anion exchange chromatography, specifically using a 1 mL HiTrap Q-Sepharose HP column (Amersham Pharmacia Biosciences). In Figure 15 the elution profiles for the metallated and apo forms of both proteins are shown as detected at 254 nm absorbance. No significant differences were observed in the anion exchange elution volumes between the apo and metallated forms of the

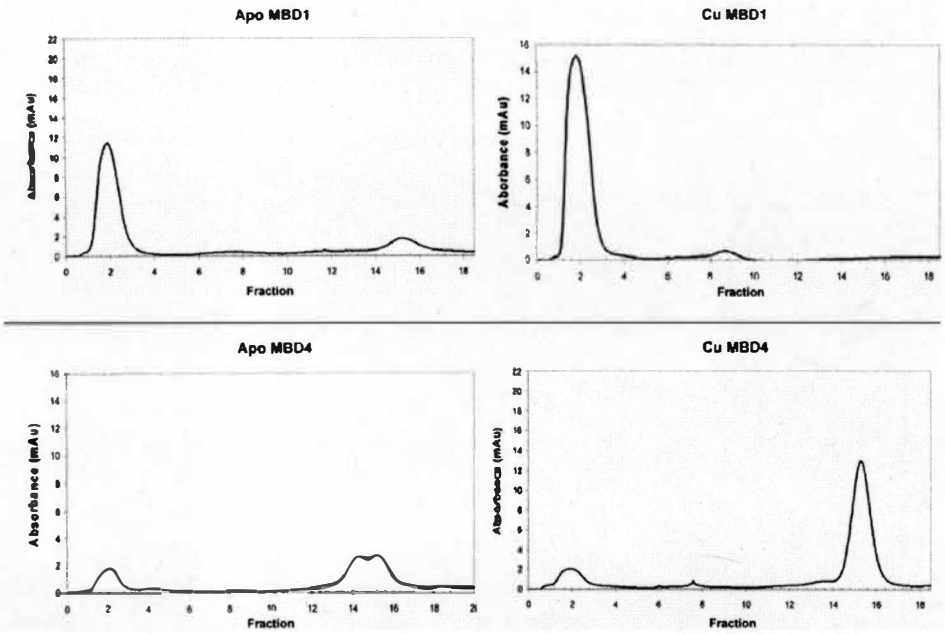

Figure 15. Separation of MBD1 and MBD4 using Anion Exchange Chromatography

In control studies consistent results were obtained determining that MBD1 eluted from the column in fractions 2-3 and MBD4 eluted in fractions 14-17. Elution volumes were not affected by the presence of copper.

proteins, although UV absorbance values for the metallated proteins were significantly increased over those of apo proteins with similar concentrations. For purposes of protein solubility all metallation and copper exchange experiments were performed using the buffer: 20 mM MES/Na, 150 mM NaCl, pH 6.0. In order to prevent the occurrence of excess copper present after the metallation process, a 1.0 molar equivalent was incubated with the protein followed by successive buffer exchanges for removal of any unbound metal. Both the apo and metallated stock solutions of protein for each domain were analyzed for copper content and protein concentration. The protein concentrations were determined by amino acid hydrolysis and thiol quantitation (Thiol and Sulfide Quantitation Kit by Molecular Probes). Protein concentrations were estimated within 5% difference between the two methods; the results obtained by thiol determination were selected for further calculations. The copper content of the protein containing fractions was analyzed using ICP-MS. Protein concentration and copper content of the control reactions are listed in Table 2. The ability of each protein to readily bind copper was demonstrated through high percentage of metal bound protein present after incubation with the metal for 10 minutes. During the metallation process 97% of MBD1 and 84% of MBD4 acquired copper. Four volumes of buffer were exchanged immediately after metallation using a 10 mL Amicon ultra filtration cell theoretically leaving less than 0.01 μM of free Cu(I) in solution.

	Concentration μM			
Control	[MBD1]	[Cu-MBD1]	[MBD4]	[Cu-MBD4]
Cu-MBD1	8.68	8.41	0	0
Apo MBD1	7.97	5.08	0	0
Cu-MBD4	0	0	11.92	10.00
Apo MBD4	0	0	8.43	0.77

Table 2. Copper Content and Protein Concentration of Control Tests

The observed increase in absorbance at 254 nm of metal-bound proteins over apo proteins allowed for the copper transfer experiments to be qualitatively monitored through UV measurement during FPLC separation of the proteins. In Figure 16 the absorbance profiles collected during the anion exchange chromatography separation of the proteins are depicted for the forward (Cu-MBD1 → MBD4) and reverse (Cu-MBD4 → MBD1) reactions. The profiles show a decrease in absorbance for the copper donor as its quantity of metallated protein is reduced and

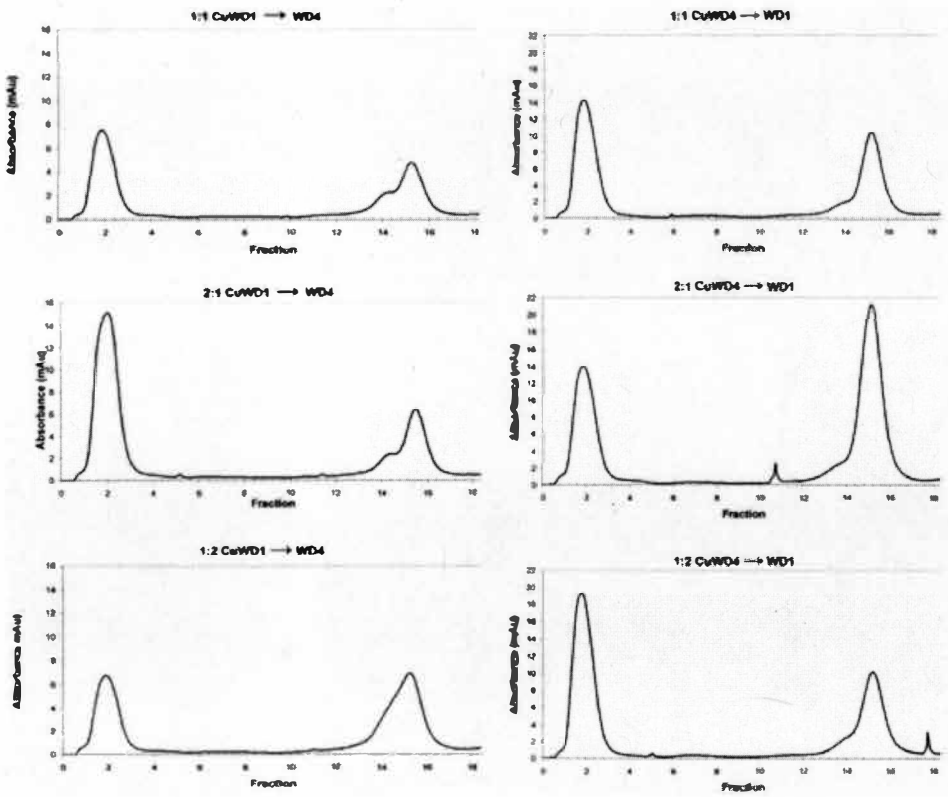

Figure 16. FPLC Absorbance Profiles for Copper Exchange MBD1 and MBD4 Separation

a corresponding increase in absorbance for the copper acceptor when compared to the initial absorbance states shown in Figure 15.

Additionally the copper exchanges of differing molar ratios between the donor and acceptor reinforce a pattern of copper exchange. When the quantity of copper donor was doubled and acceptor kept the same, the absorbance peak for the donor retained a high value and the acceptor peak increased only slightly indicating little additional copper was exchanged in the presence of excess donor. Conversely when the copper acceptor is doubled and the donor concentration unchanged the donor peak changed more dramatically as more copper was received during the exchange.

The copper content for each protein fraction collected after copper exchange was analyzed using ICP-MS. Samples were diluted during the analysis to reduce interferences caused by NaCl. The molar concentrations of the initial and equilibrium copper bound proteins have been calculated for the metal exchange studies. Additionally, the copper exchange constant was calculated; the copper exchange equation is given in Figure 17. Table 3 lists the copper distribution of each copper exchange experiment and the $K_{exchange}$ value. The $K_{exchange}$ values for the forward and reverse exchange reactions indicative equilibrium was reached in the allotted time before separation of the proteins was conducted. The average $K_{exchange}$ value is 0.69 as determined by a linear regression analysis.

$$K_{exchange} = \left| \frac{[WD1]_{total}}{[Cu-WD1]_{eq}} - 1 \right| \Bigg/ \left| \frac{[WD4]_{total}}{[Cu-WD4]_{eq}} - 1 \right|$$

Figure 17. Calculation of the Copper Exchange Constant

	Initial Concentration μM				Equilibrium Concentration μM		
Cu Donor	[MBD1]	[Cu-MBD1]	[MBD4]	[Cu-MBD4]	[Cu-MBD1]	[Cu-MBD4]	$K_{exchange}$
MBD1	8.68	8.41	8.43	0.77	4.54	3.95	0.80
MBD1	8.68	8.41	8.43	0.77	2.76	3.74	0.92
MBD1	8.68	8.41	8.43	0.77	3.17	3.99	0.89
MBD4	7.97	5.08	11.92	10.00	3.74	4.44	0.67
MBD4	7.97	5.08	11.92	10.00	3.82	4.43	0.64
MBD4	7.97	5.08	11.92	10.00	3.34	4.44	0.82
MBD1	17.36	16.82	8.43	0.77	8.57	3.74	0.82
MBD1	17.36	16.82	8.43	0.77	7.20	3.03	0.79
MBD1	17.36	16.82	8.43	0.77	6.88	3.03	0.85
MBD4	7.97	5.08	23.84	20.00	4.48	11.18	0.69
MBD4	7.97	5.08	23.84	20.00	3.82	10.21	0.81
MBD4	7.97	5.08	23.84	20.00	3.94	10.35	0.78
MBD1	8.68	8.41	16.86	1.54	2.41	3.99	0.81
MBD1	8.68	8.41	16.86	1.54	2.44	3.60	0.69
MBD1	8.68	8.41	16.86	1.54	2.12	3.50	0.81
MBD4	15.94	10.16	11.92	10.00	5.52	3.82	0.89
MBD4	15.94	10.16	11.92	10.00	4.67	3.75	1.11
MBD4	15.94	10.16	11.92	10.00	5.44	4.45	1.15

Table 3. Copper Exchange Distribution Between MBD1 and MBD4

Protein concentration calculations are based total reaction volume (1.2 mL), stock concentrations (listed in Table 2), and the injection volume (1 mL) for each copper exchange separation.

CHAPTER IV

DISCUSSION

The objective of this study was to isolate and characterize the N-terminal MBD1 and MBD4 of Wilson disease protein and further determine their ability to reversibly exchange copper between. The disease-causing missence mutation of MBD1, G85V, was also to be investigated in comparison to the wild type.

While the G85V was successfully cloned into *E. coli* expression vectors pET-21d and pET-24d, the protein could not readily be expressed and therefore comparisons between the mutant and wild type of MBD1 could not be accomplished. The mutant is likely to be misfolded and less stable than the wild type creating many difficulties in successfully obtaining soluble recombinant protein. The application of a fusion tag for expression of the mutant could increase protein yields. Fusion tags are a common method of improving solubility and correct folding of recombinant proteins through fusion to another protein which is highly soluble. Another approach to improving the expression would be examining incubation temperatures more thoroughly to include 15°C and 20°C. Lower temperatures reduce the rate of expression and can increase the protein yield as a result.

In contrast to MBD1 mutant, both MBD1 and MBD4 yielded successful results when expressed in *E coli* under optimized conditions. The proteins were each purified to homogeneity and characterized by high resolution gel filtration, MALDI mass spectrometry, isoelectric focusing, and amino acid hydrolysis. Copper transfer studies were conducted on MBD1 and MBD4.

High resolution gel filtration studies of MBD1 and MBD4 yielded single Gaussian absorbance profiles for each protein. Molecular mass determinations based

upon high resolution gel filtration using two different columns consistently overestimated the size of the MBDs. This result is not unexpected since molecular mass calibration curves using gel filtration are less accurate for low mass proteins.

The purified proteins were each characterized using MALDI mass spectrometry for verification of the expected molecular masses based upon the known amino acid sequences. Mass spectrometry data determined both proteins were of the expected mass within an experimental error of $\pm$ 4 Da. Additionally MBD4 was also present in the methionine-processed form.

The isoelectric points of several of the purified MBDs of WDP were measured. Although the experimentally determined isoelectric points of the were generally found to have lower values than predicted, with the exception of MBD4, discrepancies in the exact sequence of the recombinant proteins can account for these differences. The sequences of the metal-binding domains have been determined by sequence alignment with known copper binding ATPases. Different research groups have reported some variation in the assignment of the exact beginning and end of the domains; generally the differences are only a few additional or omitted residues on each end. If these variant residues are charged the isoelectric points of the domains will be slightly different. For purposes of examining copper transfer between the MBDs based upon surface charge these differences should not effect the metal-binding site environment since the N- and C- termini of the protein are located on the opposite side of the molecule as shown in Figure 3.

The differences in isoelectric point values between MBD1 and MBD4 were the basis for testing whether the two domains could exchange copper. Additionally the difference in isoelectric points allowed for an easy separation of the proteins by anion exchange chromatography. Anion exchange control experiments were

conducted to examine the elution times of the apo and metallated forms of both proteins. MBD1 consistently eluted in the early fractions possible and was concluded not to bind to the column. No changes in elution time were noted between apo and metallated MBD1. A single Gaussian peak was observed during the elution of MBD1 with increase absorbance due to the presence of copper. Apo MBD4 showed two overlapping elution peaks in control tests. As the quantity of metallated MBD4 increased the first peak diminished and the second peak increased. These results indicate the apo and metallated forms of MBD4 might be interacting with the anion exchange resin in different manner. Elution times of MBD4 were unaffected by whether the protein was metallated with the protein eluting in fractions 14-17 consistently. MBD4 also showed an absorbance increase with copper present.

The buffers used for the copper exchange experiments and subsequent anion exchange separation were each treated with Chelex-100 resin to minimize background levels of copper. Inevitably the MBDs acquired some copper during purification and the metal exchange studies. The ability of the proteins to strip copper from the buffers is indicative of their high affinity for the metal. MBD1 exhibited an increased instability over MBD4, MBD6, and MBD5-6. Determining the optimum storage conditions (i.e. buffer, pH, salt concentration) for MBD1 would likely correct this problem.

The distinct properties of the two MBDs predicted the possibility for copper exchange to occur and indeed when examined *in vitro* this was found to be the case. The electrostatic surface differences between the MBDs are thought to enable the proper positioning of the proteins in order for the copper exchange event to occur. Experimental results indicate equilibrium is reached quickly, within less than 5 minutes. An attempt was made to replicate physiological conditions by keeping

copper concentrations low within the estimated physiological concentrations (Tsivkovskii, 2002) with upper limits of 20 μM. The transfer experiments were conducted as near to physiological pH as the stability of the MBDs allowed. However, MBD1 exhibited increased instability and insolubility as pH neared 7. This is most likely due to the isoelectric point (6.7) of MBD1 being near this pH. As a result, the metal transfer studies were performed at pH 6. Temperature considerations for the experimental design were limited to the environment of the anaerobic glove box utilized during the study. Although 37°C would have been preferred to simulate physiological conditions, the glove box was only able to maintain a steady temperature of 18°C for the transfer experiments and the resources to set up an incubator within the glove box were inaccessible.

Although copper exchange was observed between the individual domains MBD1 and MBD4 of WDP *in vitro* whether this is the same case *in vivo* with the native protein remains to be seen. Currently the structure of the N-terminal metal-binding region of WDP is not known and therefore the relative arrangement of the six MBDs within the protein is also unresolved. The linking loops between the MBDs of WDP have differing lengths with the longest being between and the fourth and fifth domains and the shortest between the fifth and sixth domains (Arnesano, 2001b). The ability of the MBDs to exchange copper would be dependent on their surface charges as well as their faculty to properly align for exchange to occur requiring a certain degree of mobility within the N-terminal metal-binding region of WDP. The changes in the conformation of N-terminal metal-binding region of WDP with increasing molar ratios of copper reported indicate some movement may occur (DiDonato, 2000). MBD4 would appear to be a good candidate for participation in domain-domain copper exchange since it possesses the most potential mobility of the

domains based upon the length of its linking loops. In support of MBD4 playing a role in transferring copper to some or all of the other domains are the results of yeast two-hybrid studies examining Atox1 interactions with the individual MBDs of WDP (van Dongen, 2004). The strongest interactions were detected between the metallochaperone and MBD4 and to a lesser degree with MBD1 and MBD2.

The determination of MBD1 and MBD4 being capable of exchanging copper *in vitro* suggests that domain-domain copper transfer within WDP is plausible under the proper conditions and further investigations will be required to determine if these conditions do indeed exist *in vivo*. Determination of the existence of domain-domain copper exchange events within the native state of WDP will require some careful planning. The next step will require synthesis of all six MBDs individually and additionally as one unit with the domains linked together. Protein-protein interaction detection methods such as two-hybrid analysis, cross-linking, fluorescence energy transfer (FRET) or surface plasmon resonance (SPR) could be employed to detect the exchange. However, the small size of the domains and relative proximity to each other will complicate the results of these methods which are more commonly utilized to detect interactions between molecules that are not attached. It is likely more than one approach of analyzing protein-protein interactions will be required to interpret the results properly. In combination analyzing domain-domain interactions the structure of the N-terminus metal-binding region could be determined using NMR techniques for analysis of which MBDs are likely to interact based on spatial orientation.

Assuming domain-domain copper exchange occurs within WDP prompts the question of whether preferential acceptor –donor pairs exist. Similarly to studies performed with Atox1 (Larin, 1999; van Dongen, 2004; Walker, 2004), a single

copper loaded MBD could incubated with apo MBD1-6 and examined in terms of if copper exchange occurred and which MBD accepted the copper. Although this approach may not be conclusive in itself, as a single MBD will have greater accessibility than in the native state, some insight may be provided as to which MBDs are more likely to interact.

The implications of copper exchange taking place between MBDs within WDP may point to a new mechanism of regulation for the protein. Several studies have suggested that the first four MBDs may serve a separate function than the latter two MBDs. Is so, a model of protein regulation using the ability of the domains to transfer copper between each other for purposes of monitoring activities such as copper transport activity of the intramembrane metal-binding site CPC, catalytic phosphorylation activity, and interaction with the metallochaperone Atox1 could explain the functional non-equivalence of the individual MBDs of WDP. Under this model copper would be delivered via Atox1 to one of the first four domains (Larin, 1999). The subsequent transfer of copper to one of the latter two domains would be dependent of upon the quantity of copper present effecting the regulation of copper transport activity (Forbes, 1999), catalytic phosphorylation activity (Huster, 2003), and intracellular protein trafficking (Cater, 2004). For MBD5 and MBD6 have been indicated to be crucial for these events to occur while MBDs one through four have either been identified as not necessary or undetermined as to their roles in these copper dependent activities. If the MBDs of WDP are capable of exchanging copper many of the protein's copper mediated activities could be affected.

BIBLIOGRAPHY

Amaravadi R., Glerum D., Tzagoloff A. 1997. Isolation of a cDNA Encoding the Human Homolog of COX17, a Yeast Gene Essential for Mitochondrial Copper Recruitment. Hum Genet 99 3: 329-333.

Anastassopoulou I., Banci L., Bertini I., Cantini F., Katsari E., Rosato A. 2004. Solution Structure of the Apo and Copper(I)-Loaded Human Metallochaperone HAH1. Biochemistry 43:13046-13053.

Arnesano F., Banci L., Bertini I. 2001. Solution Structure of Cu(I) and Apo Forms of the Yeast Metallochaperone Atx1. Biochemistry 40: 1528-1539.

Arnesano F., Banci L., Bertini I., Cantini F., Ciofi-Baffoni S., Huffman D., O'Halloran T. 2001. Characterization of the Binding Interface between the Copper Chaperone Atx1 and the First Cytosolic Domain of Ccc2 ATPase. J Biol Chem 276 44: 41365-41376.

Arnesano F., Banci L., Bertini I., Ciofi-Baffoni S., Molteni E., Huffman D., O'Halloran T. 2002. Metallochaperones and Metal-Transporting ATPases: A Comparative Analysis of Sequences and Structures. Genome Research 12:255-271.

Banci L., Bertini I., Ciofi-Baffoni S., Huffman D., O'Halloran T. 2001. Solution Structure of the Yeast Copper Transporter Domain Ccc2a in the Apo and Cu(I)-loaded States. J Biol Chem 276 11:8415-8426.

Banci L., Bertinin I., Del Conte R., D'Onofrio M., Rosato A. 2004. Solution Structure and Backbone Dynamics of the Cu (I) and Apo Forms of the Second Metal-Binding Domain of Menkes Protein ATP7A. Biochemistry 43:3396-3403.

Baneyx, F. 1999. Recombinant Protein Expression in *Escherichia coli.* Current Opinions in Biotechnology 10:411-421.

Bradford M. 1976. A Rapid and Sensitive Method for the Quantitation of Microgram Quantities of Protein Utilizing the Principle of Protein-Dye Binding. Anal Biochem 72:248-254.

Brewer G., Yuzbasiyan-Gurkan V. 1992. Wilson Disease. Medicine 71 3:139-164.

Bull P., Thomas G., Rommens J., Forbes J., Cox D. 1993. The Wilson Disease Gene is a Putative Copper-transporting ATPase Similar to the Menkes Disease Gene. Nat Genet 5: 344-350.

Bull P., Cox D. 1994. Wilson Disease and Menkes Disease: New Handles on Heavy-metal Transport. Trends in Genetics 10 7:246-252.

Camakaris J., Voskoboinik I., Mercer J.F. 1999. Molecular Mechanisms of Copper Homeostasis. Biochem Biophys Res Commun 261: 225-232.

Cater M., Forbes J., LaFontaine S., Cox D., Mercer J. 2004. Intracellular Trafficking of the Human Wilson Protein: The Role of the Six N-Terminal Metal Binding Sites. Biochem J 380:805-813.

Cobine P., George G., Winzor D., Harrison M., Mogahaddas S., Dameron C. 2000. Stoichiometry of Complex Formation between Copper(I) and the N-Terminal Domain of the Menkes Protein. Biochemistry 39:6857-6863.

Culotta V., Klomp L., Strain J., Casareno R., Krems B., Gitlin J. 1997. The Copper Chaperone for Superoxide Dismutase. J Biol Chem 72 38: 23469-23472.

Danks D., Stevens B., Campbell P., Gillespie J., Walker-Smith J., Blomfield J. Turner B. 1972. Menkes' Kinky Hair Syndrome. Lancet 1:1100-1102.

Danks D. 1995. Disorders of Copper Transport. In: C.R. Scriver A. L., Beaudet W. V., Sly D. Valle (Eds), Metabolic Basis of Inherited Disease, McGraw-Hill, New York, 2211-2235.

DiDonato M., Narindrasorasak S., Forbes J., Cox D., Sarkar S. 1997. Expression, Purification, and Metal Binding Properties of the N-terminal Domain from the Wilson Disease Putative Copper-transporting ATPase (ATP7B). J Biol Chem 272 52:33279-33282.

DiDonato M., Hsu H., Narindrasorasak S., Que L., Sarkar B. 2000. Copper Induced Conformational Changes in the N-terminal Domain of the Wilson Disease Copper-transporting ATPase. Biochemistry 39:1890-1896.

DiDonato M., Zhang J., Que L., Sarkar B. 2002. Zinc Binding to the NH_2-terminal Domain of the Wilson Disease Copper-transporting ATPase. J Biol Chem 277 16:13409-13414.

Ellman, G. 1959. Tissue Sulfhydryl Groups. Arch Biochem Biophys 82: 70-77.

Fleischer B. 1903. Zwei weitere Fälle von Grünliche Verfärbung der Kornea. Klin Mbl Augenheilk 41:489-91.

Forbes J., Hsi G., Cox D. 1999. Role of Copper-Binding Domain in the Copper Transport Function of ATP7B, the P-type ATPase Defective in Wilson Disease. J Biol Chem 274 18:12408-12413.

Gitschier J., Moffat B., Reilly D., Wood W., Fairbrother W. 1998. Solution Structure of the Fourth Metal-binding Domain From the Menkes Copper-transporting ATPase. Nat Struct Biol 5:47-54.

Hamza I., Schaefer M., Klomp L., Gitlin J. 1999. Interaction of the Copper Chaperone HAH1 with the Wilson Disease Protein is Essential for Copper Homeostasis. PNAS 96 23:13363-13368.

Hamza I., Prohaska J., Gitlin J. 2003. Essential Role for Atox1 in the Copper-Mediated Intracellular Trafficking of the Menkes ATPase. PNAS 100 3:1215-1220.

Hou Z., Narindrasorasak S., Bhushan B., Sarkar B., Mitra B. 2001. Functional Analysis of Chimeric Proteins of the Wilson Cu(I)-ATPase (ATP7B) and ZntA, a Pb (II)/Zn(II)/Cd(II)-ATPase from *Escherichia coli.* J Biol Chem 276 44:40858-40863.

Huffman D., O'Halloran T. 2000. Energetics of Copper Trafficking Between the Atx1 Metallochaperone and the Intracellular Copper Transporter, Ccc2. J Biol Chem 275 25:18611-18614.

Huffman D., O'Halloran T. 2001. Function, Structure, and Mechanism of Intracellular Copper Trafficking Proteins. Annu Rev Biochem 70:677-701.

Hung I., Suzuki M., Yamaguchi Y., Yuan D., Klausner R., Gitlin J. 1997. Biochemical Characterization of the Wilson Disease Protein and Functional Expression in the Yeast *Saccharomyces cerevisiae.* J Biol Chem 272 34:21461-21466.

Huster D., Lutsenko S. 2003. The Distinct Roles of the N-terminal Copper-binding Sites in Regulation of Catalytic Activity of the Wilson's Disease Protein. J Biol Chem 278 34:32212-32218.

Iida M., Terada K., Sambongi Y., Wakabayashi T., Miura N., Koyama K., Futai M., Sugiyama T. 1998. Analysis of Functional Domains of Wilson Disease Protein (ATP7B) in *Saccharomyces cerevisiae*. FEBS Letters 428:281-285.

Johnson B., Hecht M. 1994. Recombinant Proteins Can Be Isolated from *E. coli* Cells by Repeated Cycles of Freezing and Thawing. Bio/Technology 12:1357-1360.

Kayser B. 1902. Ueber einen Fall fon angeborener grünlicher Verfärbung der Kornea. Klin Mbl Augenheilk 40:22-25.

Klomp L., Lin S., Yuan D., Klausner R., Culotta V., Gitlin J. 1997. Identification and Functional Expression of HAH1, a Novel Human Gene Involved in Copper Homeostasis. J Biol Chem 272 14: 9221-9226.

Larin D., Mekios C., Das K., Ross B., Yang A., Gilliam T. 1999. Characterization of the Interaction between the Wilson and Menkes Disease Proteins and the Cytoplasmic Copper Chaperone, HAH1p. J Biol Chem 274 40:28497-28504.

Lieberman R., Rosenzweig A. 2004. Metal Ion Homeostasis. Comprehensive Coordination Chemistry II 8:195-211.

Lee J., Peña M., Nose Y., Thiele D. 2002. Biochemical Characterization of the Human Copper Transporter Ctr1. J Biol Chem 277 6:4380-4387.

Linder, M. Biochemistry of Copper. Plenum Press, New York, 1991.

Linder, M., Hazegh-Azam M. Copper Biochemistry and Molecular Biology. 1996. Am J Clin Nutr 63: 797S-811S.

Lutsenko S., Kaplan J. 1995. Organization of P-Type ATPases: Significance of Structural Diversity. Biochemistry 34:15607-15613.

Lutsenko S., Petrukhin K., Cooper M., Gilliam C., Kaplan J. 1997. N-terminal Domains of Human Copper-Transporting Adenosine Triphosphates (the Wilson's and Menkes Disease Proteins) Bind Copper Selectively *in Vivo* and *in Vitro* with Stoichiometry of One Copper Per Metal-binding Repeat. J Biol Chem 272 30:18939-18944.

Lutsenko S., Efremov R., Tsivkovskii R., Walker J. 2002. Human Copper-Transporting ATPase ATP7B (The Wilson's Disease Protein): Biochemical

Properties and Regulation. Journal of Bioenergetics and Biomembranes 34 5:351-362.

Mandal A., Yang Y., Kertesz T., Argüello J. 2004. Identification of the Transmembrane Metal Binding Site Cu^{+}-Transporting P_{IB}-Type ATPases. J Biol Chem 279 52:54802-54807.

Menkes J., Alter M., Steigleder G., Weakley D., Sung J. 1962. A Sex-linked Recessive Disorder With Retardation of Growth, Peculiar Hair, and Focal Cerebral and Cerebellar Degeneration. Pediatrics 29 5: 764-779.

Mitra B., Sharma R. 2001. The Cysteine-rich Amino-terminal Domain of ZntA, a Pb(II)/Zn(II)/Cd(II)-translocating ATPase from Escherichia coli, is Not Essential for Its Function. Biochemistry 40:7694-7699.

Morris S., Revill W., Staunton J., Leadlay P. 1993. Purification and Separation of Holo- and Apo- Forms of *Saccharopolyspora erythraea* Acyl-carrier Protein Released from Recombinant *Escherichia coli* by Freezing and Thawing. Biochem J 294:521-527.

Novagen. 2003. 10^{th} Edition pET system Manual.

O'Halloran T., Culotta V. 2000. Metallochaperones, an Intracellular Shuttle Service for Metal Ions. J Biol Chem 275 33:25057-25060.

Payne A., Gitlin J. 1998. Functional Expression of the Menkes Disease Protein Reveals Common Biochemical Mechanisms Among the Copper-transporting P-type ATPases. J Biol Chem 273 6:3765-3770.

Paynter J., Grimes A., Lockhart P., Mercer J. 1994. Expression of the Menkes Gene Homologue in Mouse Tissues Lack of Effect of Copper on the mRNA Levels. FEBS Letters 351:186-190.

Peña M., Lee J., Thiele D. 1999. A Delicate Balance: Homeostatic Control of Copper Uptake and Distribution. J Nutr. 129: 1251-1260.

Petris M., Voskoboinik I., Cater M., Smith K., Kim B., Llanos R., Strausak D., Camakaris J., Mercer J. 2002. Copper-Regulated Trafficking of the Menkes Disease Copper ATPase is Associated with Formation of a Phosphorylated Catalytic Intermediate. 277 48:46736-46742.

Pufahl R., Singer C., Peariso K., Lin S., Schmidt P., Fahrni C., Culotta V. Penner-Hahn J., O'Halloran T. 1997. Metal Ion Chaperone Function of the Soluble Cu(I) Receptor Atx1. Science 278:853-856.

Puig S., Lee J., Lau M., Thiele D. 2002. Biochemical and Genetic Analyses of Yeast and Human High Affinity Copper Transporters Suggest a Conserved Mechanism for Copper Uptake. J Biol Chem 277 29:26021-26030.

Rae T., Schmidt P., Pufahl R., Culotta V., O'Halloran T. 1999. Undetectable Intracellular Free Copper: The Requirement of a Copper Chaperone for Superoxide Dismutase. Science 284: 805-808.

Ralle M., Cooper M., Lutsenko S., Blackburn N. 1998. The Menkes Disease Protein Binds Copper Via Novel 2-Coordinate Cu(I)-cysteinate in the N-terminal Domain. J Am Chem Soc 120:13525-13526.

Rosenzweig A. 2001. Copper Delivery by Metallochaperone Proteins. Acc Chem Res. 34:119-128.

Scheinberg H., Gitlin D. 1952. Deficiency of Ceruloplasmin in Patients with Hepatolenticular Degeneration (Wilson's Disease). Science 116:484-485.

Singh R., Blättler W., Collinson A. 1993. An Amplified Assay for Thiols Based on Reactivation of Papain. Anal Biochem 213: 49-56.

Solioz M., Odermatt A., Krapf R. 1994. Copper Pumping ATPases: Common Concepts in Bacteria and Man. FEBS Letters 346:44-47.

Strausak D., La Fontaine S., Hill J., Firth S., Lockhart P., Mercer J. 1999. The Role of GMXCXXC Metal Binding Sites in the Copper-induced Redistribution of the Menkes Protein. J Biol Chem 274 16:11170-11177.

Strausak D., Howie M., Firth S., Schlicksupp A., Pipkorn R., Multhaup G., Mercer J. 2003. Kinetic Analysis of the Interaction of the Copper Chaperone Atox1 with the Metal Binding Sites of the Menkes Protein. J Biol Chem 278 23:20821-20827.

Suzuki M., Aoki T. 1994. Impaired Hepatic Copper Homeostasis in Long-Evans Cinnamon Rats: Reduced Biliary-excretion of Copper. Pediatric Res 35 5:598-601.

Suzuki M., Gitlin J. 1999. Intracellular Localization of the Menkes and Wilson's Disease Proteins and their Role in Intracellular Copper Transport. Pediatrics International 41:436-442.

Terada K., Nakako T., Yang X., Iida M., Aiba N., Minamiya Y., Nakai M., Sakaki T., Miura N., Sugiyama T. 1998. Restoration of Holoceruloplasmin Synthesis in LEC Rat After Infusion of Recombinant Adenovirus Bearing WND cDNA. J Biol Chem 273 3: 1815-1820.

Terada K., Aiba N., Yang X., Iida M., Nakai M., Miura N., Sugiyama T. 1999. Biliary Excretion of Copper in LEC Rat after Introduction of Copper Transporting P-Type ATPase, ATP7B. FEBS Letters 448: 53-56.

Toyoshima C., Nakasako M., Nomura H., Ogawa H. 2000. Crystal Structure of the Calcium Pump of Sarcoplasmic Reticulum at 2.6 Å Resolution. Nature 405:647-655.

Tsay M., Fatemi N., Narindrasorasak S., Forbes J., Sarkar B. 2004. Identification of the "Missing Domain" of the Rat Copper-transporting ATPase, ATP7B: Insight into the Structural and Metal Binding Characteristics of its N-terminal Copper-Binding Domain. Biochimica et Biophysica Acta 1688:78-85.

Tsivkovskii R., MacArthur B., Lutsenko S. 2001. The Lys^{1010}-Lys^{1325} Fragment of the Wilson's Disease Protein Binds Nucleotides and Interacts with the N-terminal Domain of This Protein in a Copper-dependent Manner. J Biol Chem 276 3:2234-2242.

Tsivkovskii R., Eisses J., Kaplan J., Lutsenko S. 2002. Functional Properties of the Copper-transporting ATPase ATP7B (The Wilson's Disease Protein) Expressed in Insect Cells. J Biol Chem 277 2:976-983.

Vanderwerf S., Cooper M., Stetsenko I., Lutsenko S. 2001. Copper Specifically Regulates Intracellular Phosphorylation of the Wilson's Disease Protein, a Human Copper transporting ATPase. J Biol Chem 276 39:36289-36294.

van Dongen E., Klomp L., Merkx M. 2004. Copper-dependent Protein-protein Interactions Studied by Yeast Two-hybrid Analysis. Biochem Biophys Res Commun 323: 789-795.

Voskoboinik I., Strausak D., Greenough M., Brooks H., Petris M., Smith S., Mercer J., Camakaris J. 1999. Functional Analysis of the N-terminal CXXC Metal-binding

Motifs in the Human Copper-transporting P-type ATPase Expressed in Cultured Mammalian Cells. J Biol Chem 274 31:22008-22012.

Vulpe C., Levinson B., Whitney S., Packman S., Gitschier J. 1993. Isolation of a Candidate Gene for Menkes Disease and Evidence That It Encodes a Copper-transporting ATPase. Nat Genet 3:7-13.

Vulpe C, Packman S. 1995. Cellular Copper Transport. Ann Rev Nutr 15:293-322.

Walker J., Tsivkovskii, R., Lutsenko S. 2002. Metallochaperone Atox1 Transfers Copper to the NH_2-Terminal Domain of the Wilson's Disease Protein and Regulates its Catalytic Activity. J Biol Chem 277 31: 27953-27959.

Walker J., Huster D., Ralle M., Morgan C., Blackburn N., Lutsenko S. 2004. The N-terminal Metal-binding Site 2 of the Wilson's Disease Protein Plays a Key Role in the Transfer of Copper from Atox1. J Biol Chem 279 15:15376-15384.

Wernimont A., Huffman D., Lamb A., O'Halloran T., Rosenzweig A. 2000. Structural Basis for Copper Transfer by the Metallochaperone for the Menkes/Wilson Disease Proteins. Nat Struct Biol 7:766-771.

Wernimont A., Yatsunyk L., Rosenzweig A. 2004. Binding of Copper(I) by the Wilson Disease Protein and Its Copper Chaperone. J Biol Chem 279 13:12269-12276.

Wilson S. 1912. Progressive Lenticular Degeneration: A Familial Nervous Disease Associated With Cirrhosis of the Liver. Brain 34 295-507.

Xiao Z., Loughlin F., George G., Howlett G., Wedd A. 2004. C-Terminal Domain of the Membrane Copper Transporter Ctr1 from *Sacchromyces cerevisiae* Binds Four Cu(I) Ions as a Cuprous-Thiolate Polynuclear Cluster: Sub-femtomolar Cu(I) Affinity of Three Proteins Involved in Copper Trafficking. J Am Chem Soc 126:3081-3090.

Yamaguchi Y., Heiny M., Gitlin J. 1993. Isolation and Characterization of a Human Liver cDNA as a Candidate Gene for Wilson Disease. Biochem Biophys Res Comm 197:271-277.

Yamaguchi Y., Heiny M., Suzuki M., Gitlin J. 1996. Biochemical Characterization and Intracellular Localization of the Menkes Disease Protein. PNAS 93:14030-14035.

Yuan D, Stearman R, Dancis A, Dunn T, Beeler T, Klausner R. 1995. The Menkes/Wilson Disease Gene Homologue in Yeast Provides Copper to a Ceruloplasmin-like Oxidase Required for Iron Uptake. PNAS 92:2632-2636.